LyTEC-R-00-005

LyTec LLC

FINAL REPORT

TASK 2

ASSESSMENT OF MCRM BOOST ASSIST FROM ORBIT FOR DEEP SPACE MISSIONS

Order No. H-30549D / Modification 2

April 6, 2000 through May 15, 2000

Submitted to:

National Aeronautics and Space Administration
George C. Marshall Space Flight Center
Marshall Space Flight Center, AL 35812

Attn: John Cole / Manager, Space Transportation Research
Advanced Space Transportation Program

Submitted by:

LyTec LLC
P. O. Box 1581
1940 Elk River Dam Rd
Tullahoma, TN 37388

May 25, 2000

1.0 TABLE OF CONTENTS

LIST OF TABLES

Page

LIST OF FIGURES

Page

1.0 INTRODUCTION

1.1 Scope of Work

The work reported on herein was undertaken by LyTec at the request of NASA Marshall Space Flight Center, Advanced Space Transportation Programs. This effort was incorporated as an add-on task to LyTec's existing contract under contract Order No. H-30549D.

The Scope-of-Work under this task directed LyTec to look at a novel NASA mission scenario for deep space probes and planetary missions. This scenario (described in Section 1.3) encompassed boosting a vehicle from Low-Earth-Orbit into a deep space trajectory. Boost propulsion being supplied by an externally powered Magnetohydrodynamic Chemical Rocket Motor, the MCRM. Power to drive the MCMR is through energy beamed from an orbiting power station. The principal advantage to this approach over past concepts on utilization of MHD augmented propulsion lies in the simple fact that the additional weight burden associated with the power supply for the MHD system is not on-board.

The specific expertise area within the scope of work to which LyTec was to provide analysis and assessments was evaluation of the magnetohydrodynamic (MHD) accelerator. LyTec staff has conducted past studies of this device and its use to augment chemical rocket propulsion. [1-7] The results of these studies formed the basis for initiation of this reported effort and the computational methods developed previously were made available to allow detailed calculations of the performance of the MHD accelerator.

Under the direction of NASA, LyTec was given guidance by which this work was to be pursued.[1] Fundamental to this guidance was the direction:

> - *Do not constrain your study to the current state-of-the-art but rather consider optimistically what technology advancements can provide in ten to twenty years* -

This positive philosophy guided the work that is reported herein and our conclusions are predicated upon this philosophy. Consideration of advanced technology breakthroughs in the areas of superconductors; high strength, lightweight materials; thermal management systems; power conditioning, power controls; and rectenna specific power; allow for a very positive assessment of the MCMR unimpeded for the underlying constraint to these types of propulsion systems, namely increased weight.

Our work was structured with two analytical tasks:

1. Mission and Configuration Analysis
2. MCMR Performance Evaluations and Mapping

Details on the sub-efforts of these tasks are provided in Table I which is a re-statement of the Statement-of-Work (SOW) under contract. LyTec was able to address all sub-efforts as defined in the SOW with a fair amount of detail consistent the resources of this contract.

[1] Private communications between LyTec research staff and Dennis Bushnell, NASA LaRC and Les Johnson, NASA MSFC related to this study.

TABLE I

STATEMENT OF WORK

Task - Title	Task Description
1.0. Mission and Configuration Analysis	Under this task, LyTec will conduct background studies to determine/define criteria related to the mission and the system configuration as is required to perform the technical analysis of the MCRM orbit-boost-to-deep space under Task 2.0. • LyTec will conduct background and literature searches to familiarize key researchers on the mission and NASA objectives. • LyTec staff will coordinate/communicate with NASA experts and visionaries to determine a comprehensive definition of the mission & system configuration. • LyTec staff will communicate with NASA, National Laboratories and outside experts to determine the state-of-the-art and capabilities/capacities of the different system components comprising the overall system and the mission concept. • LyTec will set on paper a *"ground-rules criteria set"* as is needed to support the analytical efforts of Task 2.0. This set will express the underlying technical assumptions/definitions used, system and component specs (size, capacity , operational) and other unknown factors; underlying the analysis - to serve as a means of judging the project results and its conclusions. (This effort/foundation will be critiqued with NASA technical management during the early part of project to assure NASA needs are met and that synergism exists in the problem definition.)
2.0 MCRM Performance Mapping	This task is the focal task for the project. Under this task, analysis will be performed to evaluate the MCRM and its unique sub-component requirements to determine the performance and capability of this unique system to meet the mission requirements. • LyTec will utilize existing in-house computational resources to analyze the operation and performance of the MCRM as constrained to the mission definition. • LyTec will perform analysis of propulsion measures (Isp, acceleration, acceleration times, mission times, etc.) of the MCRM system encompassing trade-off studies on operational variables; i.e., weights, fuel load, fuel type, energy conversion and efficiency measures, etc. • LyTec will produce graphs, maps, and other visuals that portray key propulsion and mission performance measures for the mission/system concept that can be used to guide NASA in future initiatives toward this concept.
3.0. Management and Reporting	Under this task, all project management and reporting will be accomplished. This task will serve as a focal point for conduct of all contractual matters and direct communications with the NASA project management. • A Final Report will be written documenting work on each task, reporting on conclusions drawn from the work, and providing recommendations for future efforts.

1.2 Background

The idea for employing magnetohydrodynamic (MHD) plasma acceleration for advanced propulsion systems has been recognized for decades. A class of small scale, electric propulsion devices have arisen from this including MPD and Hall thrusters. These thrusters have flown and are principally employed for satellite station keeping and deep space probes.

Larger scale MHD augmented propulsion systems are under research within NASA ASTP. This work extends to applications for single stage, earth-to-orbit vehicles and orbital boost to escape velocity for planetary (Mars mission) and deep space exploration. Within ASTP's initiatives, a myriad of MHD propulsion schemes are under evaluation including the MHD augmented

Chemical Rocket Motor, the MHD slip stream accelerator, the MHD self-excited Pulse Detonation Engine (PDE), and the MHD energy by-pass scramjet engine (AJAX concept).

This report summaries some preliminary analytical efforts directed at evaluation of the MHD augmented Chemical Rocket Motor, MCRM. Of interest to in these studies were both small scale MCRMs as a competitive thruster for deep space probes and larger scale MCRM's for boosting manned/transport vehicles from orbit for near term planetary exploration.

A treatise by LyTec researchers on the first of these applications is provided in references 6 and 7. Therein, analytical studies were performed that compared the small MCRM with an all-electric propulsion system, such as, the ion engine. The findings of that work indicated that an MCRM comparable to a ion engine is an attractive alternative with capability of producing Isp from 2,700 to 4,000 seconds, thrust of between 300 and 400 Newtons, and acceleration levels from 0.2 to 2.0 milligravities. No other currently contemporary all-electric or all-chemical thruster system for deep space probe application can provide the flexibility of relatively high thrust, high specific impulse and spacecraft acceleration that appears plausible with the MCRM.

The principal area of our work under this task explored the potential use of the MCRM coupled with beamed energy for powering of the MHD accelerator. This novel concept opens up a new forum for the MHD augmented rocket allowing its use without the need for carrying on-board power supplies, i.e., a significantly reduced system weight. Furthermore, our recent work has shown that the dramatic increase the Isp that the MHD accelerator can supply to augment the rocket motor is on the order of five to ten times, depending on size. As such,

> utilization of the MCRM with beamed energy presents a opportunity to achieve the rapid acceleration from LEO to orbit escape velocity as needed to reduce mission times for planetary exploration.

The beamed energy driven MCRM concept represents an advanced propulsion system that could significantly improve space transportation capability by lending high performance thrusters for deep space missions.

1.3 The Beamed Energy Driven MCRM Mission Concept

Our studies were an assessment for NASA on the technical and feasibility of the potential use of the beamed energy driven MCRM to enhance the mission performance in orbit-boost-to-escape for deep space missions. The type of mission scenarios currently being considered by NASA as to what scheme will be employed in first/pioneering transport and manned missions to the planets, i.e., first manned mission to Mars. [8-14]

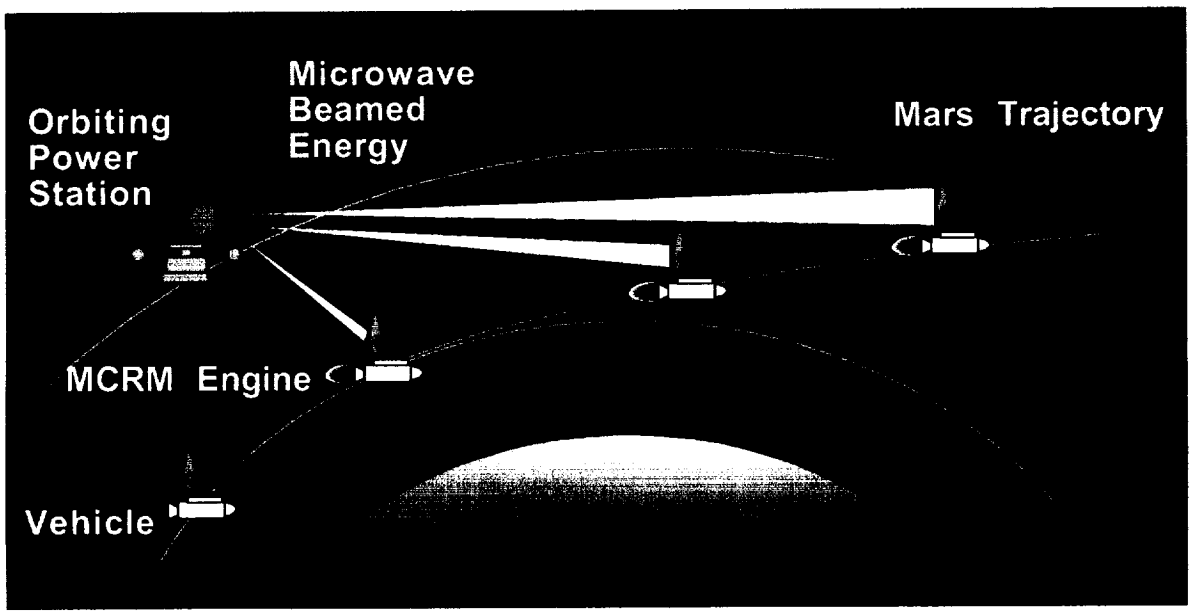

Figure 1. Space Mission Scenario - MCRM Driven By Beamed Power From An Orbiting Power Station

The mission scenario encompasses the use of beamed energy (e.g., microwave) from an orbiting power platform to an orbiting deep space vehicle/probe. Considerable studies and research are underway within NASA on both the potential, needs and operational requirements for an orbiting power station as well as methods to beam energy to space probes and process this power for propulsion.

An artist's rendition of the mission is shown in Figure 1. This mission includes microwave beamed energy from the power station being captured by a rectenna on-board the space vehicle. This beamed energy is directly converted to electric power through microprocessors with integrated rectifier arrays integral to the rectenna. The electric power produced is used to directly drive the MHD accelerator (magnet and accelerator channel).

The MHD assisted rocket firing augments the impulse of the rocket motor utilizing energy (fuel/power supply) for the MHD accelerator that is not on-board. This concept is a vision by NASA as a prospective means for enhancing vehicle acceleration to acquire higher velocity and improved trajectory - to reduce deep space mission time (such as, a manned mission to Mars).

The ability of the MCRM to augment Isp from standard rocket motor level (~450 to 500 sec) to values in the 1000 to 3000 sec range provides for the practicality of this type of mission. Beamed energy systems in the gigawatt's level has been projected which exceeds that required for the MCRM to accelerate a 80,000 kg craft at over 1.0 g based upon use of a very high power density receiving antenna.

An increase in the LEO orbital velocity of 6,000 m/sec to 10,000 m/sec is considered as that level required for achieving a Mars trajectory with viable mission time for transport and/or manned spacecraft. Consequently, accelerations in the "g's" range are needed when this is to be accomplished across a single orbital path such as shown in Figure 1. The MCRM can

provide this type of augmented performance to the rocket motor. However, limitations on the power transmission intensity and rectenna size/weight has implications on the total throughput of the MCRM that is associated with elevated levels of Isp. Limitations also exist on the distance range over which beamed power can be sustained due to transmission diffusion. In the following subsections, we review the overall mission performance/requirement with some basic principle analysis to quantify elements of the system/mission.

1.4 The MCRM Concept

Our concept for the MCMR is sketched in Figure 2. The MCRM utilizes a standard rocket motor as a driver for the propulsion system burning conventional rocket fuels such as liquid hydrogen and oxygen. In addition, a trace amount of ionization seed (0.05 to 1.0% of K or Cs by mass) is added to the combustion stream to provide the ionizable material for achieving a thermal plasma. Inlet plasma conductivity on the order of 10 mho/m is adequate to initiate the MHD processes and this level is easily achievable with thermal ionization of a seeded combustion gas.

The combustion stream is accelerated through a nozzle to achieve pre-defined state at the MHD accelerator entrance. The MHD accelerator consists of a confinement channel with electrode and insulating walls surrounded by a high field strength magnet. Electric power is supplied to the MHD accelerator from an external power source.

As the rocket stream passes through the accelerator channel, the MHD acceleration process augments the stream's kinetic energy through the principles of MHD as discussed in Section 3. The insets on Figure 2 indicate the orientation of the various MHD process vectors with the

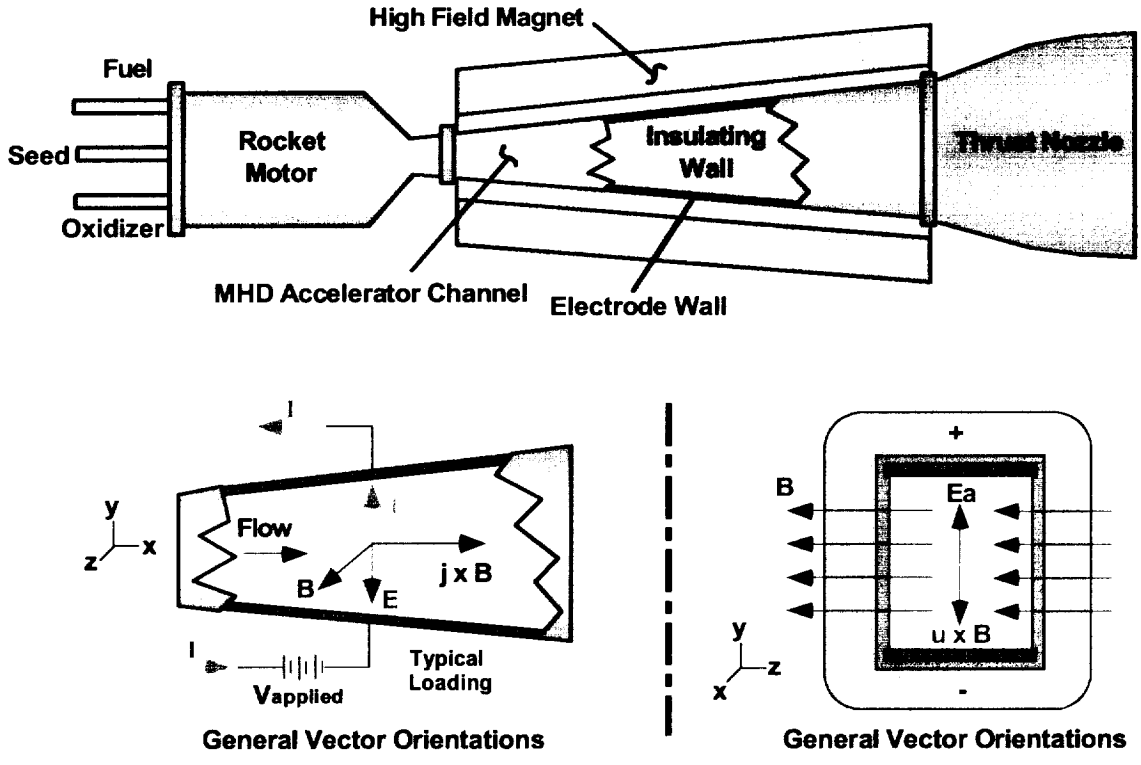

Figure 2. General Concept for the MCRM

magnetic field. We include in Figure 2 the coupling of the MHD accelerator exit with a rocket nozzle to achieve final expansion to low back pressure conditions.

This MCRM concept is currently under study by LyTec in support of NASA ASTP. We are evaluating both small and large size systems applicable to different missions. Our findings to-date have indicated that increase in Isp for a H_2-O_2 rocket to levels of 2,500 sec or more are readily achievable with the MCMR. We recognize the system trade-offs that the MCRM must met to prove its competitiveness. Paramount among these is the increased weight of the propulsion system that accompanies the inclusion of the MHD accelerator. This weight increase must be viably off-set by the increased thrust producing an increased acceleration capability.

The major system components for the MHD accelerator include the seed addition system, magnet, channel, and power supply and conditioning equipment. Studies performed in late 80's by the Department of Energy in support of the SDI's initiative for evaluation of an MHD space-based power system uncovered many new ideas for production of lightweight MHD channels. In addition, advances in HTSC show extreme promise that lightweight, superconducting, high field strength magnets will be a reality in the near future. It is our contention that development of the MCRM should keep pace this technology.

Our avid interest in the MCRM at this point in time evolves from the mission scenario being explored by NASA researchers. This mission (described in the next section) employs beamed energy as a means for providing power to the MCRM. Such an approach eliminates the need for carrying on-board power for the accelerator and therefore eliminates that excessive weight burden.

1.5 Technology Development - Status

The major components associated with the beamed energy driven MCRM include the magnet, the MHD accelerator channel, the power condition equipment, and the rectenna/power conversion system. Detailed evaluation of these systems for optimization to the MCRM was beyond the scope of this study. However, in the following topical paragraphs we touch on the needs and characteristics of these components in our review and assessment of the current and future state of development.

Magnet Technology

It has always been apparent that a superconducting magnet will be required for any space based propulsion system. This arises because the much higher power and weight required for electromagnets magnets would make conventional magnet system inefficient.

Thousands of low temperature superconducting magnets have been built and this technology is well known. However, the requirement for helium refrigeration (T below 20K) would place a large weight penalty on the system in terms of on-board cryogenics. Magnets are currently being made from 'high temperature superconductors' (temperature less than 77 K) on an experimental and early commercial basis. The goal of the national development program is to produce these conductors with an engineering current density of 10^5 amperes/cm^2.

(Engineering current density means current carrying capacity divided by the entire cross-sectional area of the conductor, including any insulation, stabilizer, substrate, etc.) This is at least an order of magnitude improvement over the low temperature superconductors but such a magnet would still require refrigeration to liquid nitrogen temperatures or below.

There is on-going development work on 'room temperature superconductors' which is extremely promising. Furthermore, the promise exists that these revolutionary conductors will permit even higher current densities to the degree that the coil mass for an MCRM propulsion system would become literally negligible. Our study assumes the availability of room temperature superconductors. However, we applied a 10^5 Amp/cm^2 current density limit to our calculations and impose a safety factor of three in the coil thickness and to provide for any structure that may be needed to support the coil internally.

A dominant factor in the weight of the magnet is the force containing structure. The maximum force to be contained increases as the square of the magnetic field flux density. This has major weight impact. The structure must be non-magnetic. Stainless steel is the most frequently used containment material in earth-based magnets. Our study followed the recommendation of the submarine propulsion work by DARPA and assumed that a composite material can be used that is non-magnetic and has the strength of stainless steel with a weight only 10% as large. Thus, the weight estimating routine used in our calculations assumed the density of stainless steel divided by 10.

Other technology issues relative to the magnet are contended to be engineering design matters. These include loads due to high accelerations during launch, magnet current control and shielding of instrumentation that is sensitive to magnetic fields.

All-in-all, LyTec is extremely optimistic as to the future of high temperature/room temperature superconducting magnets and we profess that this element of the MCRM will not be the pacing element to its fielding.

Accelerator Channel

A large body of knowledge and experience has been accumulated on design and operation of MHD generators in the United States and many other countries. MHD accelerators were built and operated in the U. S. in the 1960's. Also, an accelerator was built in Russia in this same period and the Russian accelerator test facility has been in operation since that time.[15] All of these accelerator activities were directed toward accelerating a gas for a high velocity wind tunnel. Also, all of these facilities were of the segmented Faraday type, although the LORHO facility was designed and built by the U. S. Air Force as a Hall channel but it was never operated.[16]

Operation of the accelerator to efficiently propel a vehicle in space implies operation at low pressures over at least a portion of the accelerator. At low pressures, the mean time between collisions of the free electrons and molecules becomes very large due to the low density of the gas. The Hall parameter is defined as the cyclotron frequency of the electrons times this mean time between collisions. It expresses the number of revolutions of the path of the electron due

to the magnetic field in an average time between collisions with a heavy particle. Hall parameters greater than about 4 are avoided in design of MHD generators because of the adverse effects on spatial current distribution and other characteristics (potential for axial current breakdown).

In the MHD accelerator calculations presented herein, Hall parameters as high as 100 were predicted in the far downstream, very low-pressure regimes of the channel. As such, the accelerator configuration we modeled (Faraday configuration) is in reality most inappropriate in practice. Rather, a hybrid configuration leading to a Hall accelerator in the extreme low pressure regions is probably the best approach for the MCRM design. The Hall configuration drives axial current through the channel under power to take efficient use of this high Hall field that arises from elevated Hall parameter. The theory of Hall generators and accelerators is well understood. Our computer codes are available to readily calculate the performance parameters of this type device. However, there is little, if any, experimental experience and validation of this configuration as an accelerator.

Electrode materials that will withstand the high current density and heat fluxes associated with operation of the MCRM are a major engineering issue. Most MHD devices to date, including the Russian wind tunnel at TsAGI, use highly cooled copper electrodes. Transpiration cooling is a potential solution but this likely assures a cold boundary layer and arc transport of the current between the electrode and the plasma. Transpiration cooling with inert gas has been proposed in gaseous electrode work but this would require carrying another on-board expendable.

Higher temperature operation of the electrodes may be feasible with advanced materials and transpiration cooling. Our current study considered futuristic electrode materials and cooling concepts in keeping with the theme of our study.

Power System

Power for the operation of the MCRM system under consideration comes from an orbiting power station that transmits the power to the spacecraft by microwaves. This concept has been studied for a variety of situations.[8-14] The transmission of electrical power from earth-to-space and space-to-earth by microwaves has been widely studied. The latter application was and is still being considered to evaluate the feasibility of a system of solar gathering satellites in orbit, beaming the electrical power to earth for distribution to electrical users on earth. Such a system has to compete with other sources of electrical power on economic, environmental and societal bases. In this application the frequency for the microwave power transmission is planned at about 2.45 Ghz , wavelength 0.122 m. This frequency is chosen rather than a higher one to minimize losses in transmission through the atmosphere. A space-to-space power transmission system will have no such consideration and a higher frequency should be considered.

The performance of a high gain antenna applicable to the transmission and reception of microwaves is an inverse function of wavelength, λ. That is, ideal antennas having identical D/λ, have identical gain. Thus, higher frequencies favor smaller antennas for comparable

power transmission. The limitation on how high the frequency can be depends upon the technology for generating, transmitting and receiving the microwave power.

At least one of the references [11]suggests that a 300 Ghz system is possible in the near future, although some component development will be required. At these frequencies, integrated circuits are proposed for rectifying and processing the received power. Such a system would be diversified into multiple series/parallel circuits to produce the voltages and current needed to power the magnet and accelerator electrodes.

The term "rectenna" has been used to describe the receiving antenna and integrated rectifiers. The weight of these rectenna systems subject to contemporary technology is estimated [14] at between 0.5 to1.0 kg/kW. At this level, the weight of the magnet and accelerator components are well below 1% of the total weight and are dwarfed by the rectenna weight. Thus, the weight of this rectenna appears to be the key pacing issue for the beamed energy driven MCMR as well as for other space technologies applications. Aggressive research and development to reduce the rectenna weight is needed if the concept of utilization of beamed energy for propulsion is to be realized.

An approximate equation that expresses the relationship between antenna sizes and range, as a function of wavelength, λ, is given below [10-14],

$$\eta = 1 - \exp(-A_t A_r/\lambda^2 L^2)$$

where, λ is the wavelength of the microwave power, η is the fraction of the transmitter power captured by the receiving antenna, A_t, A_r are the transmitter and receiver array areas, respectively, and L is the distance between the transmitter and receiver.

This equation is plotted in Figure 3 for an efficiency of 75% and assumes that the transmitting antenna dimension is 10 times the receiving antenna dimension. For the 300 Ghz case, the antenna sizes seem to be manageable for powering over a significant range, certainly to 1,000 Km and beyond.

Another constraint that must be considered is the power density on the antenna, especially as it dictates the losses that are released as heat in the antenna. Koert and Cha [11] have estimated that no more than 10% of the losses in the rectenna will result in heating the receiving antenna. They further calculated that losses amounting to 0.1 W/cm^2 in heating can be radiated to space if the emissivity is close to unity and the operating temperature can be as high as 373 K. This is a severe constraint and likely dictates that high power rectennas must have additional cooling.

For example, this constraint would imply a receiving antenna more than 3,000 m square for a gigawatt system. Clearly, the antenna cooling must be provided for large-scale systems. Fortunately, the fuels to be used for the working fluid can be used as the cooling media and add slightly to the thermal efficiency of the propulsion system, at some cost in weight and complexity. For an 80% efficient rectenna, the above factors indicate a 20% overall loss and a heating loss of 2% of the electric power. In the case of either a H_2/O_2 rocket engine or a water

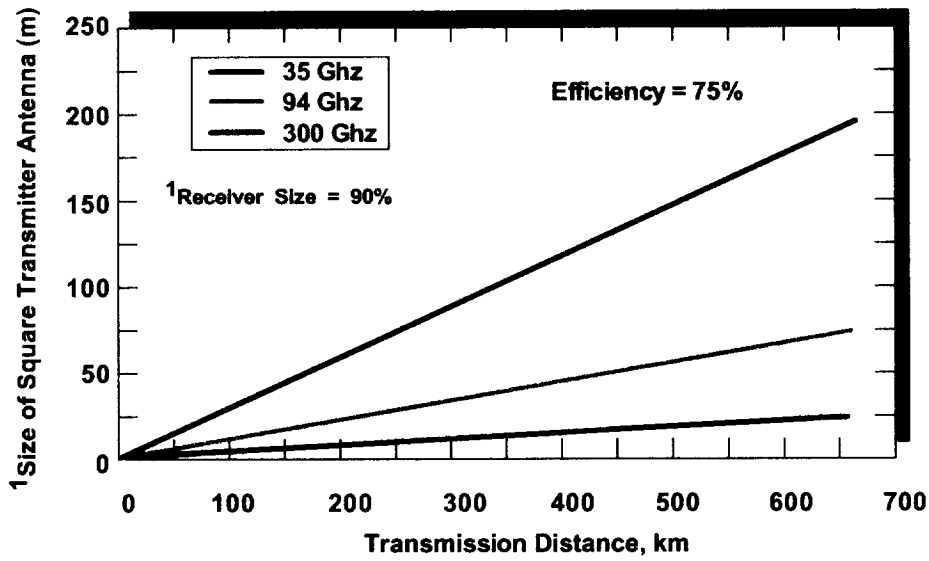

Figure 3. Required Antenna Sizes as a Function of Range to Space Vehicle

fueled system, this amount of heat can be absorbed by the working fluid and benefit the propulsion system.

Power Conditioning

There is a considerable knowledge base derived from past work on MHD generators with regard to power condition and current control for MHD devices. This knowledge base can be brought to bear for the MCRM application. The type of control system employed is not considered to be a major constraint to the system nor a major weight penalty and was therefore neglected in this study.

From the point-of-view of transmitted power, it would be highly undesirable from a weight viewpoint to take the rectified electrical power from the rectenna, convert it back to alternating current, transform it to another voltage and then rectify it again for use by the magnet and accelerator. Instead, the integrated circuit rectifier design should be configured to produce the currents and voltages required by series and parallel combinations of individual rectifier stages.

Koert and Cha [11] have outlined the requirements for such a system but additional development work will be needed. In this regard, a disadvantage to going to the high frequencies for power transmission is revealed in that the voltage received on each dipole is scaled down with wavelength and more dipoles are needed in series to drive each rectifier.

2.0 ANALYSIS

2.1 Mission Evaluation

2.1.1 Mission Overview

The first characteristic needing definition for the general boost from orbit-to-escape mission is total power requirement. If one considers boost from LEO with an initial orbiting velocity in the 4,000 to 7,000 m/s range (variation from perigee to apogee) and escape velocity to deep space from 10,000 to 13,000 m/s, then the fundamental kinetic energy imparted to the vehicle is:

$$KE = m_v (Vesc^2 - V_{LEO}^2) / 2$$

where m_v is vehicle mass, Vesc is escape and V_{LEO} is initial velocity in LEO. As an example, for the velocity increase range required ($\Delta V \sim 6{,}000$ m/sec) and considering a mean vehicle weight of 100 mTons with a mean acceleration over a period of 60 minutes, one concludes that approximate power requirements for this mission are well in the gigawatt range; i.e.,

$$0.7 \text{ gW} < \text{Power} < 2.2 \text{ gW}$$

with accelerations between .08 and 0.25 g's and distances covered from 25,000 to 36,000 kilometers.

The extreme amount of power required to perform this mission is a fact of nature that has to be dealt with irregardless of how the mission is approached or the propulsion system of choice. A general view of the power requirement is provided in Figure 4.

The mission concept under study of using beamed energy implies that the beamed energy system must be capable of producing, transmitting, receiving, conditioning, and managing both elec-trically and thermally, this level of power. We consider this as the major engineering task that faces this specific mission and others beamed energy propulsion applications as posed by NASA. Furthermore, for the missions to prove viable the beamed energy system components that are intrinsic to the vehicle must be of very high specific power to minimize its parasitic weight an enable high acceleration.

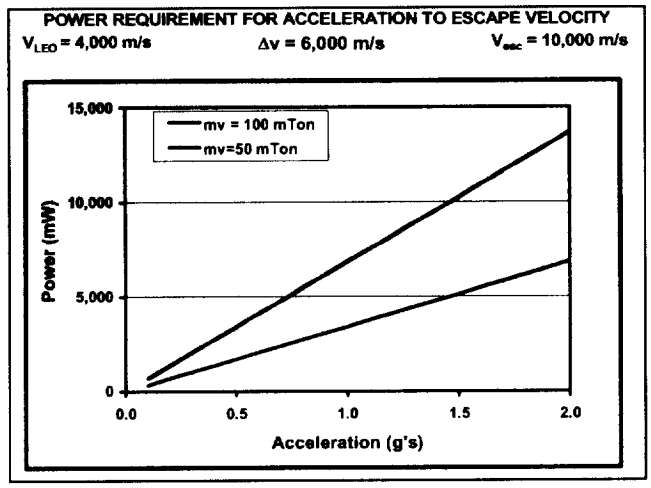

Figure 4. Power Requirement for Boost-to-Escape Mission

To better visualize the mission operational characteristics, a general analysis was performed. The propulsive force is defined according to:

$$F = \frac{ma}{g} = T = I_{sp}\,\dot{m}$$

where nomenclature is conventional (m is total instantaneous mass, a is acceleration, Isp is specific impulse and T is thrust). The mass of the total vehicle is

$$m(t) = m_i - \dot{m}\, t$$

with the fuel mass being time dependent this can be written as,

$$m_i = m_{vehicle} + m_{rectanna} + m_{fuel}$$

where $\dot{m}$ is the mass flow rate of fuel and oxidizer, or the MCRM throughput. Consideration of the dynamics yields the following expression for vehicle acceleration,

$$a = \frac{dV}{dt} = \frac{g\,F}{m_i - \dot{m}t} = \frac{g\,I_{sp}\,\dot{m}}{m_i - \dot{m}t}$$

Solving the above for velocity yields

$$V(t) = \int_0^t \frac{g\,I_{sp}\,\dot{m}}{m_i - \dot{m}t}\,dt + V_{LEO}$$

which for a constant Isp can be integrated to yield the closed form algebraic equation for instantaneous vehicle velocity,

$$V(t) = g\ I_{sp} \ln\left[\frac{m_i}{m_i - \dot{m}t}\right] + V_{LEO}$$

which along with the relations,

$$\Delta V = V_{esc} - V_{LEO}$$

$$V_f = V_{escape} = V(t_f) + V_{LEO}$$

yields,

$$\Delta V = g\,I_{sp} \ln\left[\frac{m_i}{m_i - \dot{m}t_f}\right] = g\,I_{sp} \ln\left[\frac{m_i}{m_{veh} + m_{rec}}\right]$$

Noting that the total acceleration time is the burnout time for the rocket motor, i.e.,

$$t_f = \frac{m_{fuel}}{\dot{m}}$$

The velocity expression can be solved for the initial fuel load, i.e.,

$$m_{fuel} = (m_{veh} + m_{rec})\left[\exp\left(\frac{\Delta V}{g\,I_{sp}}\right) - 1\right]$$

Carrying further, we have

$$v = \frac{ds}{dt}$$

that yields the following for distance, s, over which acceleration takes place,

$$s = \frac{g\,I_{sp}}{\dot{m}}\left\{ \left((m_{veh} + m_{rec})\right) \ln\left(\frac{(m_{veh} + m_{rec})}{m_i}\right) + \dot{m}t_f \right\} + V_{LEO}\,t$$

In our evaluation of the mission, the above equations were parametrically solved on a spreadsheet to view mission characteristics and requirements. In this exercise, we considered combination variations in rocket motor controlling parameters including specific impulse, Isp, vehicle/payload mass, m_{veh}, throughput m, and velocity increase to escape, ΔV.

For specification of the rectenna weight, a specific power parameter, ξ, was defined where

$$\xi = [\text{Power/Weight}]_{\text{rectenna}} .$$

This parameter was varied over a very broad range in our studies, i.e.,

$$2 \text{ kw/kg} < \xi < 1{,}000 \text{ kw/kg}$$

based on information provided by NASA, literature, and personal communications with experts.[2]

The total power required was derived considering the total beamed energy input with representative electrical efficiency, ηe. Electrical efficiency is of the form,

$$\eta e = \text{MHD Push Power/Total Beamed Power}$$

where ηe accounts for both power conditioning losses and MHD accelerator electrical efficiency. The MHD Push Power represents the total increase in kinetic energy of the rocket throughput across the MHD accelerator. With this formulation the rectenna weight is computed as,

$$m_{\text{rectenna}} = \text{MHD Push Power} / (\xi \, \eta e)$$

2.1.2 Scaling Studies on Mission Parameters

Figures 5 through 10 present a series of plots derived from calculations on the dynamics of the mission. These figures provide scaling measures of the effectiveness of the beamed energy driven propulsion system and give indication of the requirements that must be met for this mission to be achieved. The following tabulation presents parameters that were varied and there range in our overall study to view the mission requirements and operating characteristics.

Payload mTon	Isp sec	Mdot kg/sec	ξ kW/kg	ΔV m/sec	ηe
80	500 to 3000 sec	.1 to 100 kg/s	1 to 1000	6000 m/sec	70% to 80%

Figures 5 through 10 present calculations for three representative cases as summarized below. These cases were computed through an Isp range to map system specifications.

Case	Payload mTon	Isp sec	Mdot kg/sec	ΔV m/sec	ξ	Power gW
1	80	500 – 3,000	1	6,000	80%	.01-.54
2	80	500 – 3,000	10	6,000	80%	.11-5.4
3	80	500 – 3,000	100	6,000	70%	1.1-53.8

[2] Private Communications, Dennis Bushnell, NASA LaRC, Leik Myrabo, RPI, Richard Dickerson, JPL, Jonathan Jones, MSFC ASTP

LyTec LLC

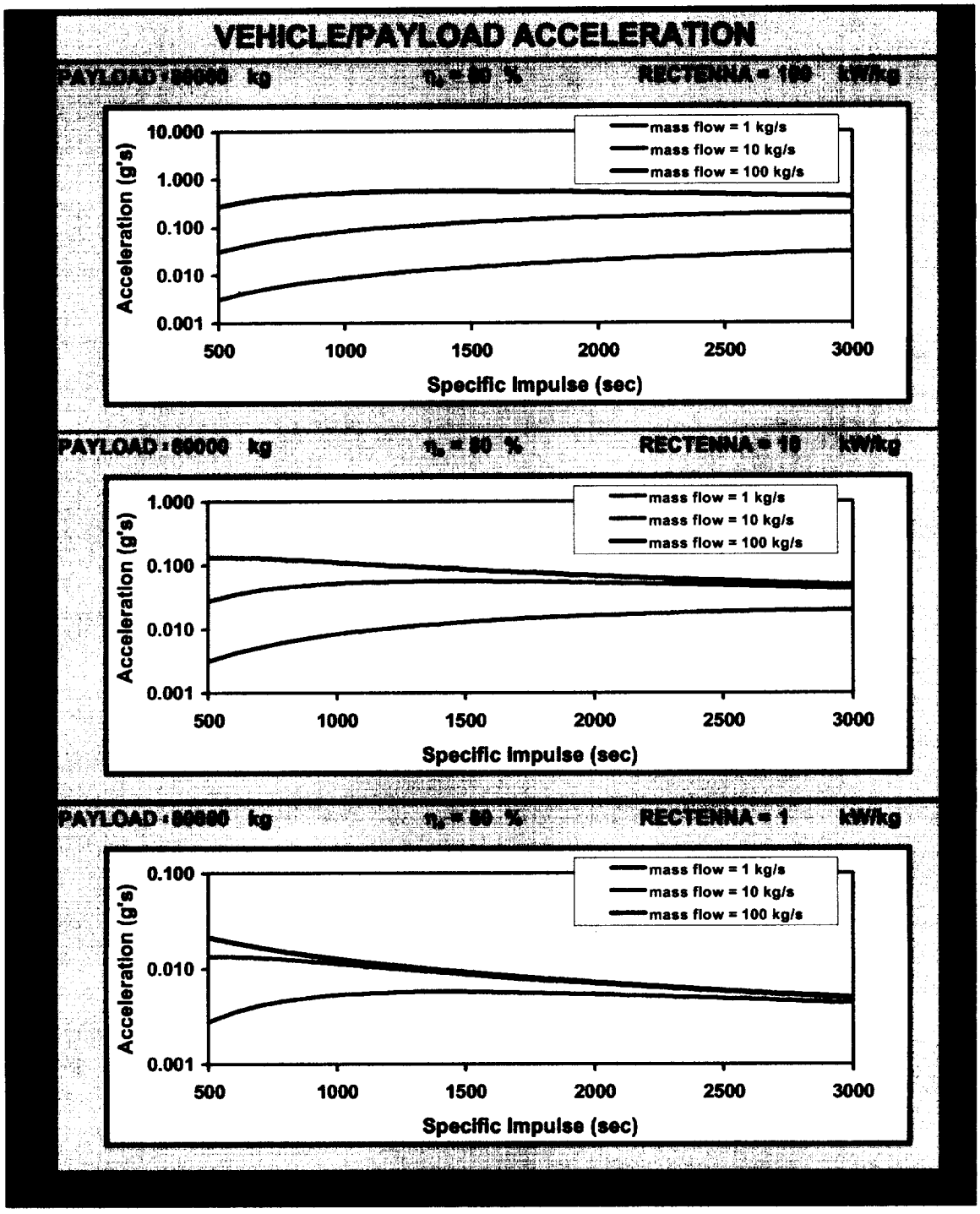

Figure 5. Mission Characteristics - Acceleration vs Isp

LyTec LLC

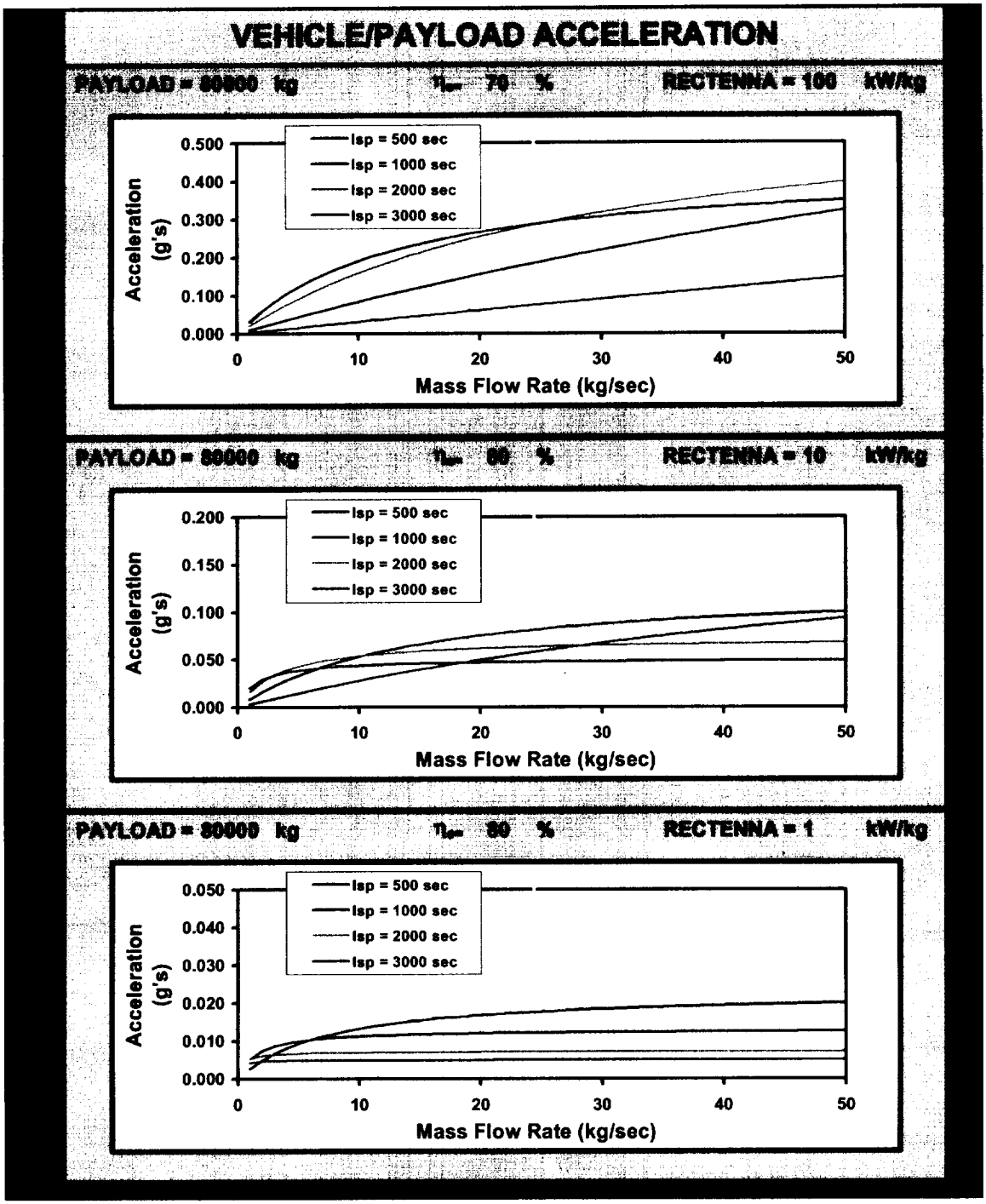

Figure 6. Mission Characteristics - Acceleration vs Throughput

LyTec LLC

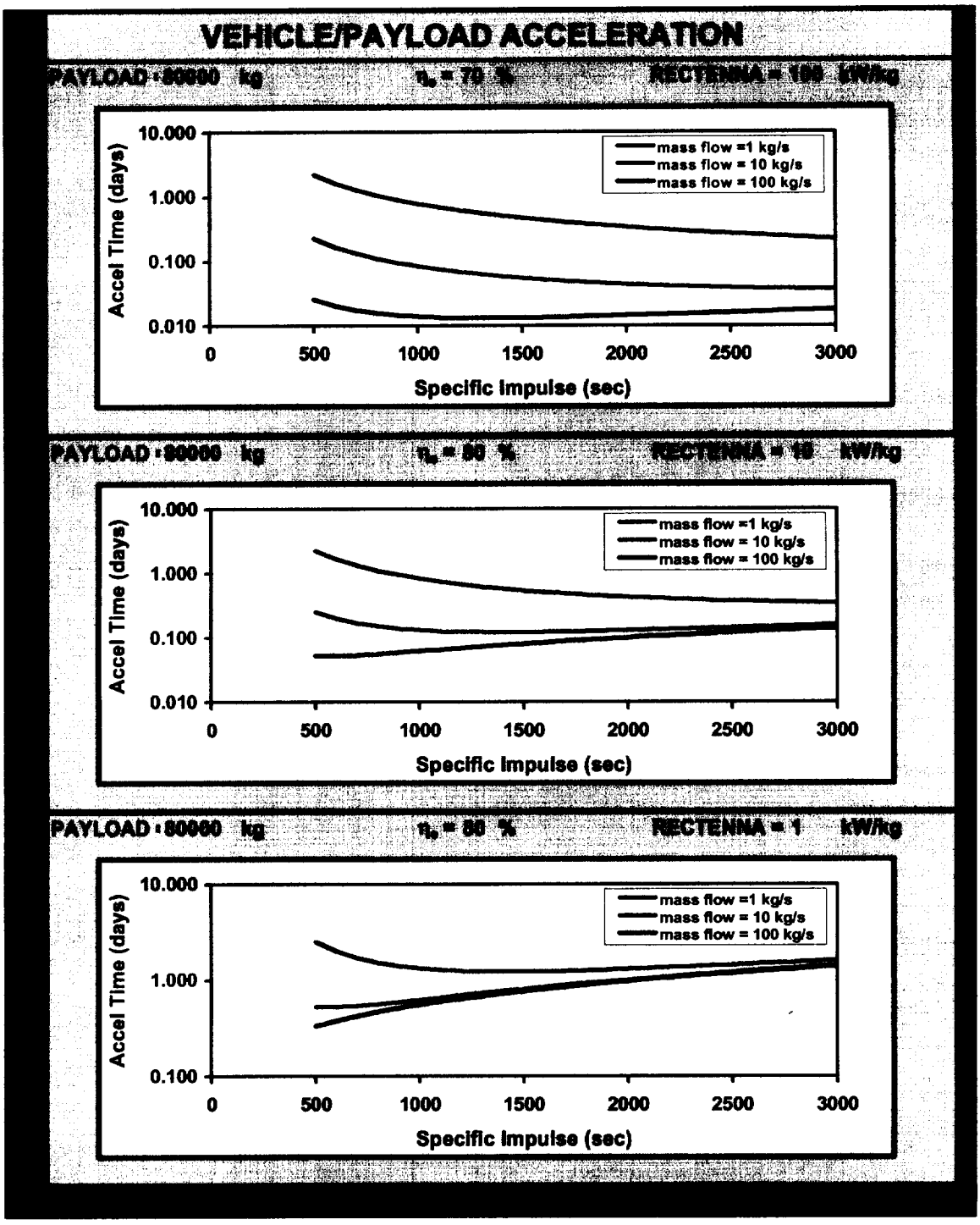

Figure 7. Mission Characteristics – Acceleration Time vs Isp

LyTec LLC

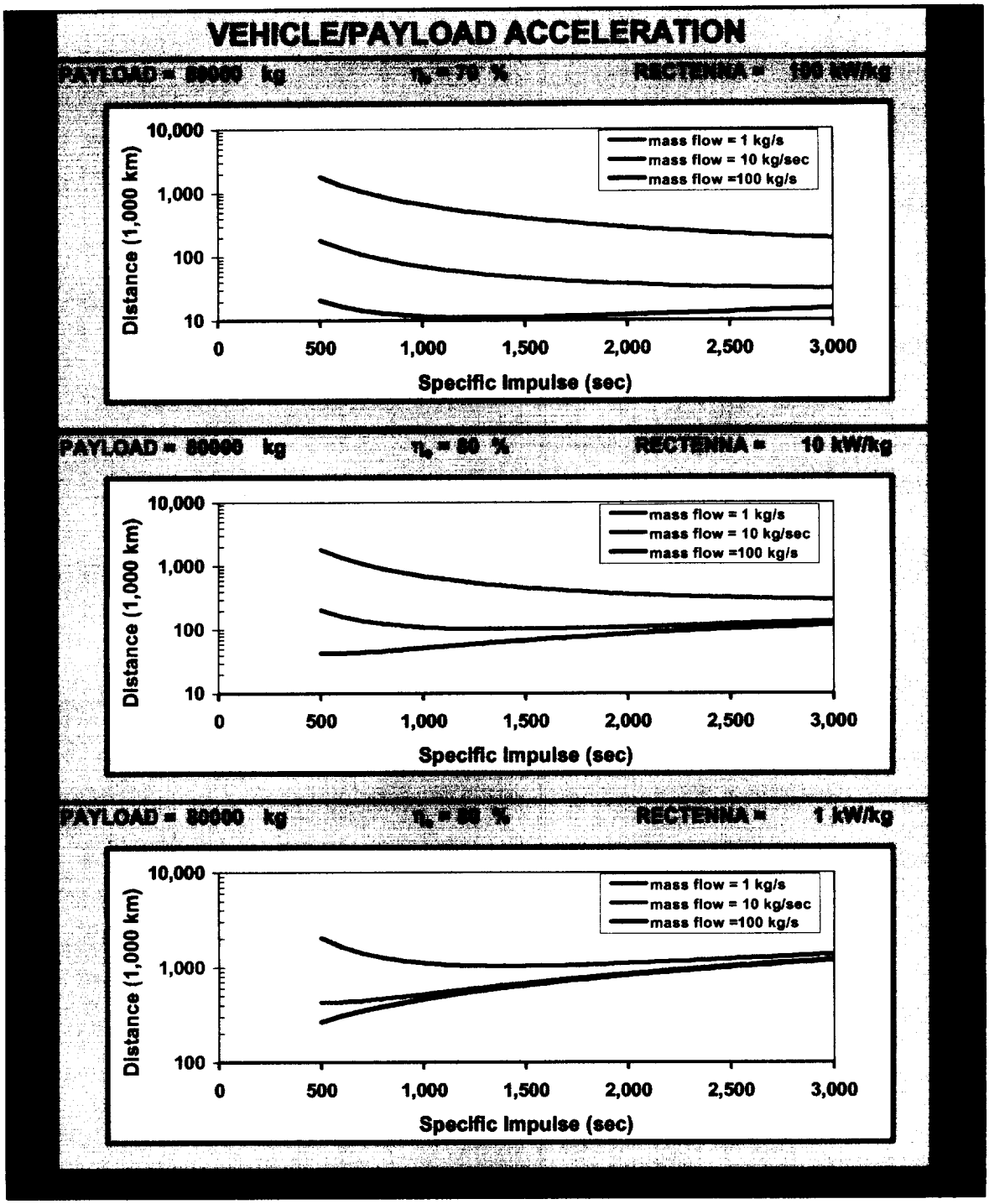

Figure 8. Mission Characteristics – Distance vs Isp

LyTec LLC

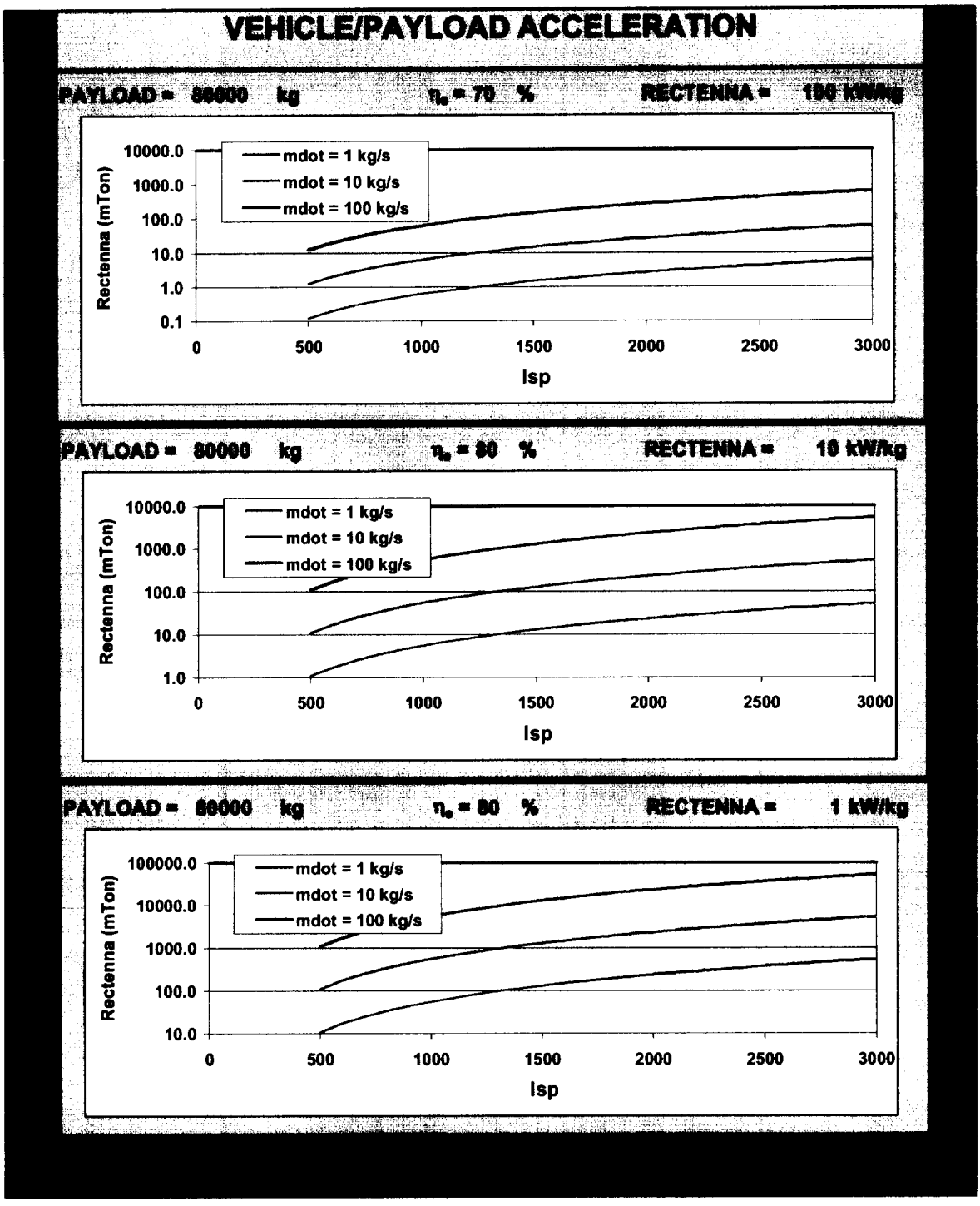

Figure 9. Mission Characteristics – Rectenna Mass vs Isp

LyTec LLC

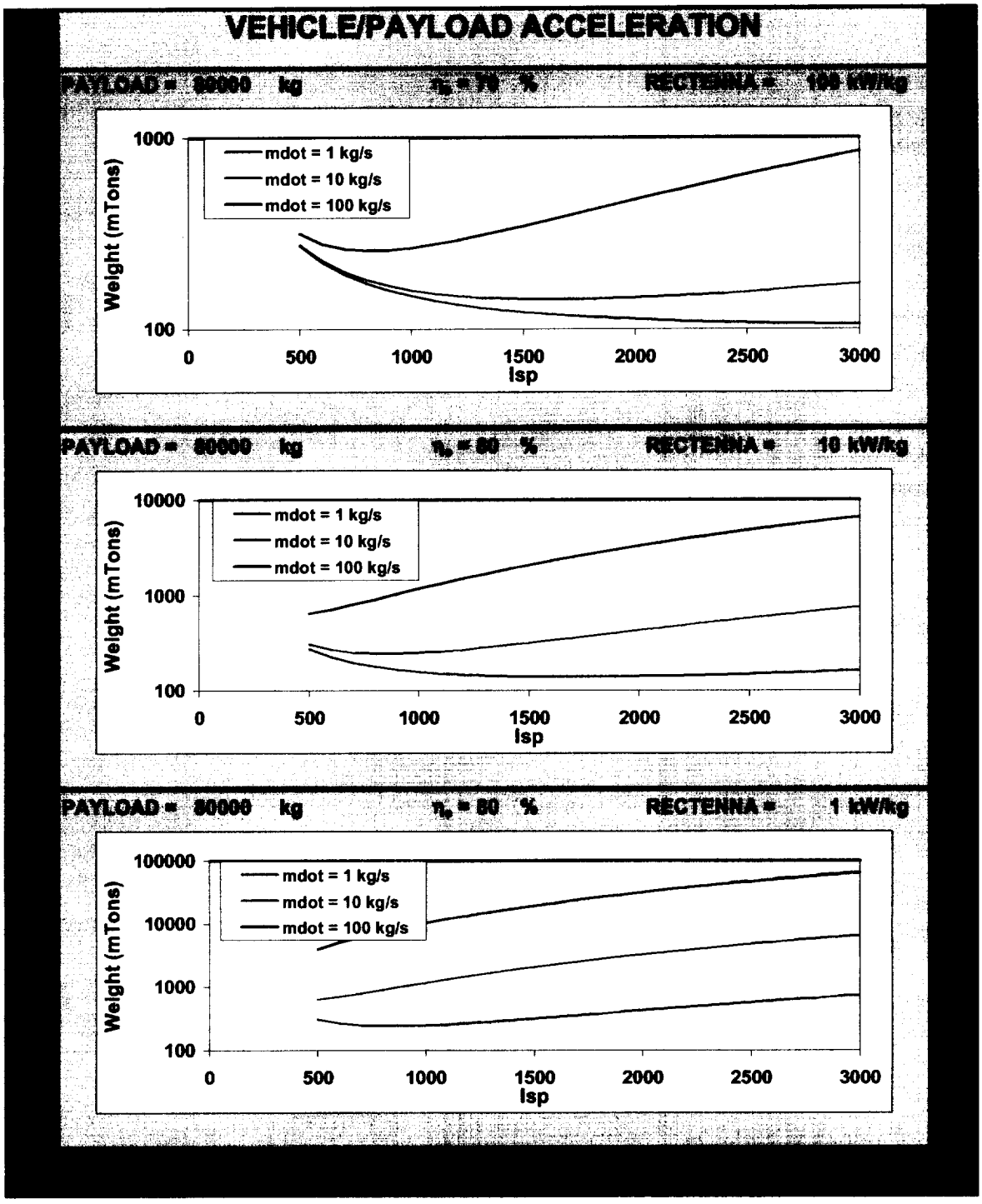

Figure 10. Mission Characteristics – Total Mass vs Isp

Figure 5 illustrates that the acceleration plausible with the beamed energy driven MCRM increases with throughput (size) and has a maximum value across the full range of Isp for each size system. For the range of rectenna power density given in the three plots, acceleration is contained at less than 1 g.

Figure 6 provides indication of the optimum size of the beamed energy driven MCRM system. Whereas the Isp lines at 500 seconds are representative of the rocket motor alone, it is seen that as Isp increases the higher lines cross under the Isp of 500 seconds line. This character moves to larger size systems as the rectenna power density is increased.

Figures 7 and 8 show the acceleration times required and beamed energy transmission distance for the cases subject to the fixed ΔV imposed.

Figures 9 and 10 illustrate the variation rectenna weight and total system weight (including fuel load).

The dominant system controlling factor that is revealed in Figures 5 through 10 is seen to be the rectenna power density. This is observed by both the change in the variation of the maps between the different cases and the magnitude of independent variables. The dominance of rectenna power density on the performance arises from variation of rectenna weight. We note the following,

$$m_{rectenna} \approx \text{Power} \approx KE_{exhaust} \approx V_e^2$$

$$I_{sp} \approx V_e$$

the rectenna weight increases with the rocket exhaust velocity, Ve, squared; whereas, the specific impulse is directly proportional to the exit velocity. This variation lends non-linearity to the performance characteristics and produces the relationship (cross-over) between the Isp lines noticeable in Figure 6.

In conclusion, the performance of the beamed energy driven propulsion system is paced by the power density of the rectenna.

- At the lower rectenna power densities reviewed, the rapid increase in the weight of the vehicle due to the rectenna size places limitation on the overall size of the MCRM system for which a significant increase in Isp over that of the fundamental rocket motor can be achieved.

- At very high rectenna power densities, a significant/revolutionary improvement in performance can be achieved by the MCRM with plausible Isp's in the 2,000 to 3,000 range.

Figure 11 summarizes these conclusions. This figure shows two maps of vehicle acceleration versus mass flow rate (size) for varying level of Isp and two distinct levels (bounds) of rectenna specific power. The lower plot represents a rectenna

specific power which has been cited in literature as being optimistically achievable for the first generation receiver, i.e., 4 kW/kg (or 0.25 kg/kw). The upper plot represents an extremely optimistic (futuristic) rectenna power density of 1Gw/kg. This level is well beyond the state-of-the-art for this device but has been quoted as the goal "range" for beamed powered earth-to-orbit vehicles.

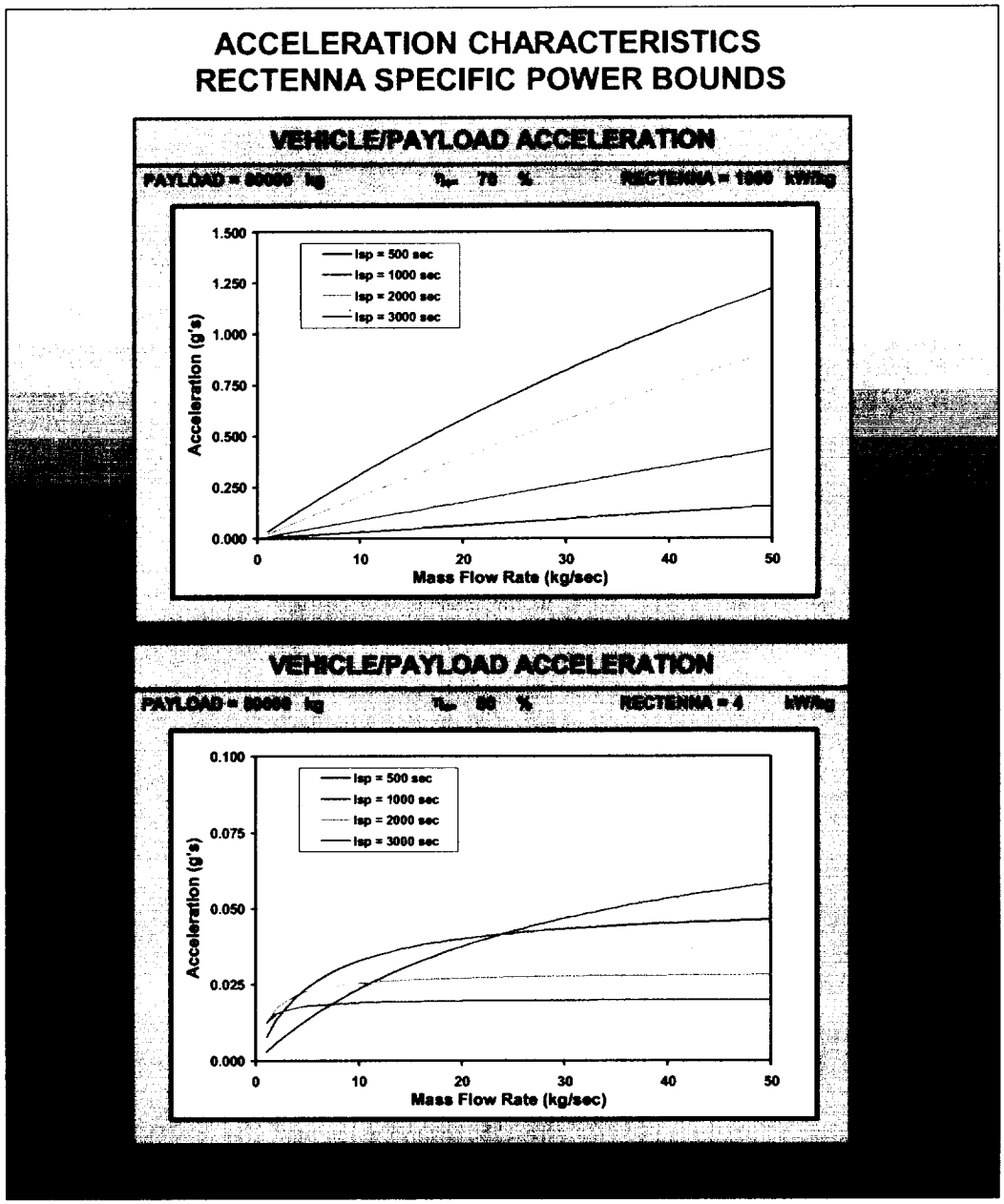

Figure 11. Vehicle Acceleration vs Size for Bounding Rectenna Specific Powers

At the lower level of rectenna specific power in Figure 11, the Isp lines cross over the 500 second line (representative of rocket motor only) in the lower left portion of the map. To the left of the cross over point represents the size of system for which the beamed energy propulsion system offers improved performance. As an example, an Isp of 3,000 seconds improves performance over the standard rocket motor for systems with throughput less than about 7.5 kg/sec. Consequently, rectenna specific power places restriction on system size.

In this upper range, it is seen that significant performance enhancement is plausible with the MCRM lending vehicle accelerations in the "g" range for large vehicles.

3.0 MHD ACCELERATOR

3.1 MHD Accelerator Operating Principles

Magnetohydrodynamics (MHD) sciences and technologies are based on the principles of electromagnetic induction in conducting fluids. In MHD devices a magnetic and an electric field are aligned orthagonal to one another and transverse to the direction of flow of a conducting fluid or plasma. This configuration is illustrated in Figure 12.

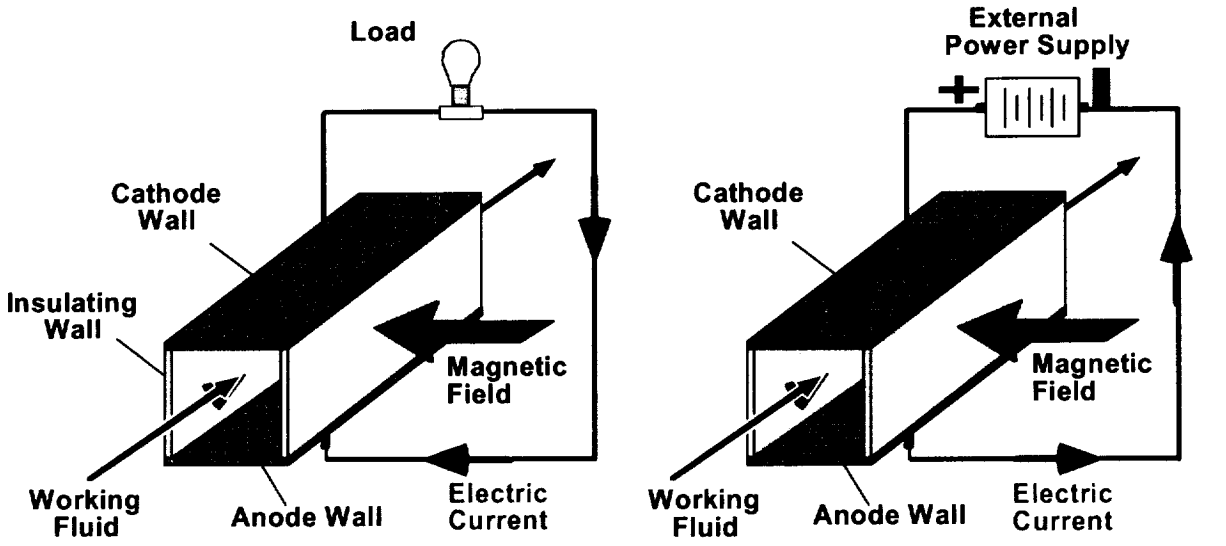

1a. Operating Principle for MHD Generator **1b. Operating Principle for MHD Accelerator**

Figure 12. Schematic Illustration of Principles of MHD

In accordance with Faraday's law of electromotive induction, the motion of the conductor (fluid/plasma) through the externally applied magnetic field induces an electromotive force (i.e., $\mathbf{E} = \mathbf{u} \times \mathbf{B}$) in the moving conductive plasma. The electric field which gives rise to an electrical potential difference developing across the fluid. The standoff potential (or voltage) that develops drives currents through the plasma when a closed circuit is externally connected to opposing electrodes walls (anode to cathode). The electric current traversing the plasma produces a Lorentz body force ($\mathbf{J} \times \mathbf{B}$) body force within the fluid, doing work on the fluid and influencing fluid motion.

In the same context as exists with conventional electromagnetic rotating machinery, two gross operating regimes for MHD devices exist. The first is the power generation mode and the second is referred to as the motor (or accelerator) mode.

Power Generation Mode (Figure 12a)

- If only a resistive electric field is impressed across the electrodes, the device functions as a generator and electrical power can be extracted. In this situation, the Lorentz body force within the fluid is directed counter to the flow direction, retarding fluid motion.

Motor or Accelerator Mode (Figure 12b)

- If an external electric field is arranged in opposition to the MHD induced electric field, then the current direction is reversed. In this case, the Lorentz force is aligned with the flow direction and the fluid is accelerated.

It is the second arrangement (Figure 12b) that is proposed for fluid acceleration augmentation in chemical rocket thrusters such as the MCRM. Here an external power supply is required with the capacity to supply a back EMF in opposition to the **u** X **B** induced EMF to force current through the plasma in the direction which accelerates the fluid.

A review of operating principles of the MHD accelerator is revealing in assessing this process for effective propulsion. Fundamental to this is Ohm's law in generalized form which describes the electrodynamics, i.e.,

$$\mathbf{j} = \sigma\left[\mathbf{E} + \mathbf{u} \times \mathbf{B}\right] - \frac{\beta}{B}(\mathbf{j} \times \mathbf{B})$$

where **j** is current density, **E** is the applied electric field, **u** is fluid velocity, **B** is magnetic field intensity and σ and β are the plasma electrical conductivity and Hall parameter respectively which are electrophysical properties of the plasma.

The simplest MHD accelerator is the Faraday configured device. In this configuration, the electrode walls are segmented to prevent axial current (Hall current) within the plasma. An illustration of the Faraday configuration is provided in Figure 13. The orientation of the Lorentz force vectors are noted in Figure 13. In general, the body force, F, that is transferred to produce flow acceleration is the integration of **J** x **B** over the channel volume.

For the Faraday configuration, Ohms law takes the following component forms,

$$J_x = 0$$

$$J_y = \frac{\sigma u B (1 - k)(1 - \Delta)}{G}$$

$$E_x = -\frac{\beta u B (1 - k)(1 - \Delta)}{G}$$

$$E_y = k u B (1 - \Delta)$$

where Jx, Jy, Ex, Ey are the Hall and Faraday components of current density and electric field respectively. Terms are included in these expressions to account for loading, boundary layer electrical losses, and flow field non-uniformity

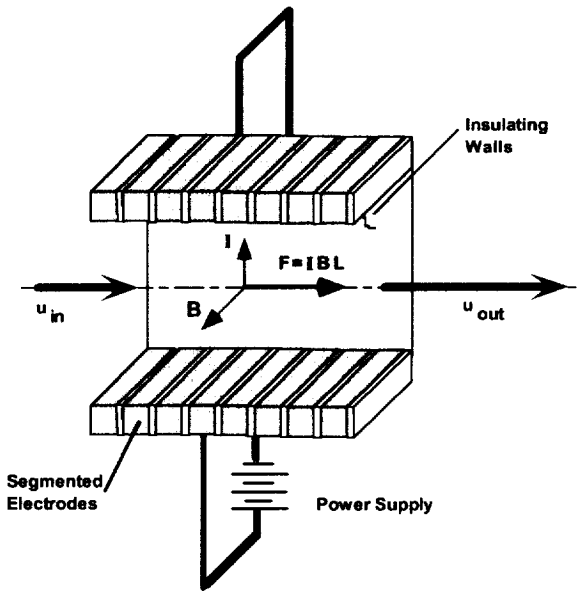

Figure 13. Faraday Configured MHD Accelerator

effects, i.e., k is the load factor defined as the ratio of the applied field (Ey) to the induced electric field (U x B), Δ is boundary layer electrical potential loss factor defined as the ratio of the voltage drop through the boundary to the overall induced voltage (Vd/uBh), and G is the Rosa non-uniformity factor.[17]

Three major specific energy terms that define the MHD accelerator process are:

$$\text{Power Input} = P = j \cdot E = \frac{\sigma u^2 B^2 k (1 - k)(1 - \Delta)^2}{G^2}$$

$$\text{Push Work} = Wp = \frac{\sigma u^2 B^2 (1 - k) (1 - \Delta)}{G}$$

$$\text{Joule Heat Dissipation} = Qj = \frac{\sigma u^2 B^2 (1 - k)^2 (1 - \Delta)^2}{G^2}$$

From energy conservation these, are related according to the following:

$$P = Wp + Qj$$

The (MHD) Push Work, Wp, is the work done on the fluid in acceleration. Joule Heat dissipation is the resistive heating of the plasma due to passage of current and is dissipative (heats up the plasma). The general expression for efficiency of the MHD accelerator process is:

$$\text{Efficiency} = \eta = \frac{W_p}{P} = \frac{G}{k (1 - \Delta)}$$

which in its simplistic form shows that the efficiency is controllable since it is inversely proportional to the load factor. Operation at a load factor near unity maximizes the portion of input power that goes into Push Work while minimizing that which goes into heating. However, at low load factors the process can be ineffective since the Push Work approaches zero as the load factor approaches 1.0.

Another unique aspect of the MHD accelerator is the disposition of the energy deposited in the plasma stream. The first law of thermodynamics can be cast for a uniform flow case to show the following:

$$\rho u \frac{d}{dx} (h + \frac{u^2}{2}) = \mathbf{u} \cdot (\mathbf{j} \times \mathbf{B}) + \frac{j^2}{\sigma} = \mathbf{j} \cdot \mathbf{E}$$

where the gas dynamic nomenclature is conventional. Here, the Joule Heat dissipation term is resistive heating and is deposited in the flow as an increase in enthalpy (temperature).

From the momentum equation;

$$\rho u \frac{du}{dx} + \frac{dp}{dx} = \mathbf{j} \times \mathbf{B}$$

or,

$$\rho u^2 \frac{du}{dx} + u \frac{dp}{dx} = \mathbf{u} \cdot (\mathbf{j} \times \mathbf{B})$$

The second expression shows that the MHD Push Work is deposited in the stream directly as kinetic energy and/or pressure depending on the channel design (area distribution). This feature of the MHD accelerator, that is,

the ability to add energy to a moving stream directly as kinetic energy,

is one of its unique characteristics that make it very attractive for a propulsion device.

We note that the efficiency of the MHD processes is most strongly influenced by the plasma conductivity. With thermal ionization, conductivity is a strong function of temperature, i.e.,

$$\sigma \approx \frac{T^a}{p^b}\ ; \text{with } 10 \le a \le 20;\ b \approx \frac{1}{2}$$

Consequently, as the load factor increases the MHD accelerator's operation will produce more combined Push Work and Joule heating. Joule heat being dissipative serves to keep the plasma temperature up thereby promoting the MHD process by keeping the plasma conductivity elevated.

From the first order principles of operation of the MHD accelerator as briefed above, it is contended that this device has the potential as an extremely effective propulsion device and can produce extremely high velocity flows. When it is used to augment a rocket engine's exhaust stream, such as our MCRM concept, it can in principle supply a means for increasing the propulsion systems Isp by orders of magnitude. This is illustrated by the calculations we preformed in this study using our MHD accelerator design and analysis computer code.

3.2 MHD Accelerator Experiments/Experience

Most previous theoretical and experimental work on MHD accelerators has concentrated on hypersonic wind tunnel applications for hypersonic testing. Among the most significant experimental programs were those of the NASA Langley Research Center [4,18] and the Air Force's Arnold Engineering Development Center.[4,16,19,20] Both programs succeeded in operating an arc-heater driven, seeded MHD accelerator and demonstrating its feasible. These programs came to an end in the late 60's. The only contemporary program on the MHD accelerator is that under NASA on the Myriah project.[21]

Similar work was also carried out in Russia by Dr. Vadim Alfyrov at the TsAGI Aerodynamic Research Center. The Russian program for developing an MHD augmented hypersonic test facility has been continuously supported to the current time. It has resulted in a operational test facility that is capable of achieving very high velocity flows [16].

Figure 14 is a map of the hypersonic test conditions simulation of this Russian facility. This map spots the hypervelocity test conditions have been achieved in practice with the MHD acceleration producing tunnel condition flows of Mach 20 and higher. This observation provides support to the technological feasibility of utilizing the MCRM in an advanced rocket propulsion system. Figure 15 is a photograph of a model in the test section of the

TsAGI MHD accellerator tunnel exhibiting the hypervelocity conditions that can be achieved.

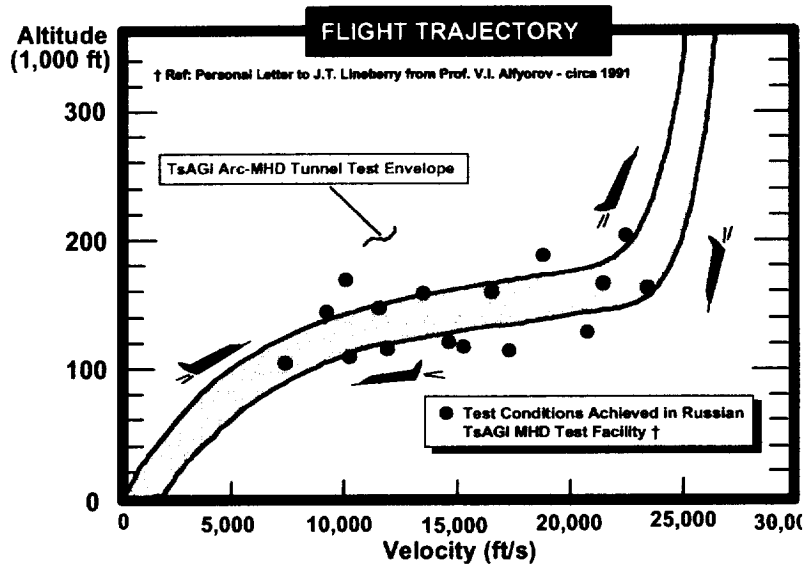

Figure14. Map of Test Points Achieved in the TsAGI MHD Accelerator Wind Tunnel

More recently there has been increasing effort in evaluation of the MHD accelerator as part of the Air Force and NASA's interest in the Russian advanced air-breathing hypersonic scramjet propulsion concept know as the "AJAX". The AJAX engine employs an MHD accelerator in the tailpipe of a scramjet combustor to add energy to the exhaust stream to control and/or control thrust. The actual concept is too com-plex for detailed discus-sion but revolves around use of MHD as a means of bypassing energy (enthalpy) around the scramjet combustor (from inlet to nozzle). [22,23]

The importance of these past and current works for space propulsion applications is associated with the successful demonstration of technical feasibility for the MHD acceleration concept and with the empirical delineation of feasible design configurations. For example, all of the successful experimental demonstrations used a segmented Faraday channel typical to that depicted in Figure 13. This configuration provides for control over the axial power distribution and can be tailored to optimize performance.

Figure15. Photo of Model in TsAGI MHD Accelerator Test Section – Hypervelocity Flow

A high static pressure plasma maintains a high collision frequency between the electrons and heavy neutral particles thereby reducing electrical conductivity. Nevertheless, a sub-scale model of the U.S. Air Force LORHO accelerator was ran in this mode with a static pressure of 0.4 atm at the accelerator inlet [20]. The system appeared promising based on limited test results. Recent studies by LyTec staff on application of the MHD accelerator to high throughput hypersonic wind tunnels are cited in references 1 through 5.

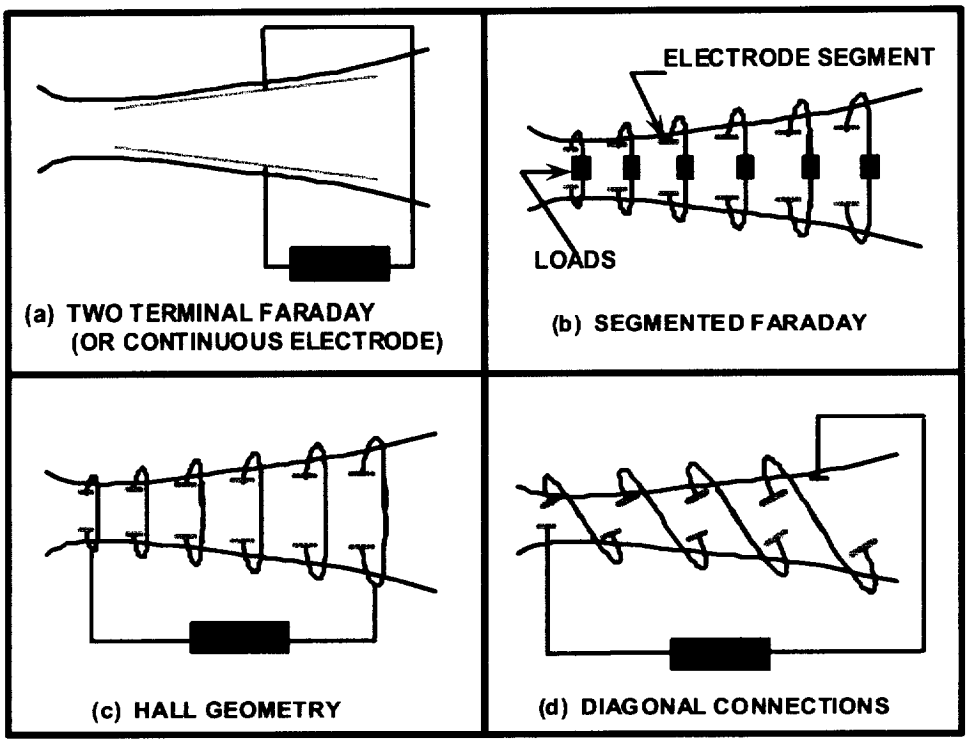

Figure16. MHD Accelerator Loading Configurations

Alternative designs/loading configurations exist which allow for optimization of the MHD accelerator/generator when the Hall parameter is high (low pressure conditions). The different loading schemes are sketched in Figure 16. The diagonal configuration depicted in Figure 16 may be considered to optimize the MHD thruster for expansion to very low back pressure. Application of the diagonal channel concept in the various hypersonic wind tunnel development programs has been limited in that a fairly high static pressure (~ 10 to 20 Atm) would be required to get the appropriate test conditions [19, 20].

The advantage of the diagonal design is associated with taking optimum advantage of the Hall effect by making electrical connections across the channel along lines of equal potential. Also, the diagonal design requires a single power supply for a reasonable length accelerator. We further note that the Hall configuration is a variation to the diagonal configuration that is optimum when the Hall parameter is extremely high, say 10 or greater.

Our MHD accelerator calculations as presented in Section 4 were made considering a Faraday configured channel. However, we note there that the extremely high Hall parameter that arises from the high expansion ratio indicates that this configuration will not be proper. LyTec foresees that MHD thruster optimization will probably best be met by a hybrid type configuration that goes from Faraday through diagonal to Hall loading scheme as the static pressure is reduced to space environment levels. We recommend this optimization as a needed future study.

4.0 RESULTS OF ANALYSIS

4.1 General Considerations

As reviewed in Section 3, the MHD augmented rocket engine concept utilizes the force created by an electrical current and a magnetic field applied mutually perpendicular to create a body force on ions in a plasma working fluid. The accelerating force is mainly transmitted to the neutral particles in the gas by collisions with ions. By this process, it is possible to provide direct and efficient increase in working fluid velocity to propel a vehicle.

Fundamental to the effectiveness of all MHD devices is the quality of the plasma working fluid. The measures of the quality of the plasma are its expansion characteristics and the level of electrical conductivity achievable. For the MCRM, working fluid is rocket motor combustion products. In our study we considered only a hydrogen/oxygen rocket engine. We also seeded the combustion gas with potassium vapor facilitate sufficient equilibrium ionization to permit efficient operation of the MHD device. (An alternative could also be considered in which the rocket engine is replaced by electrically heated water, which can be stored on board with less tankage weight.)

The base MHD accelerator calculations were made for a thermal, H_2-O_2 combustion gas plasma considering seeded at 1% potassium, by mass. Higher seeding concentration of up to a maximum of about 4 to 5 % potassium can provide higher electrical conductivity but at a cost of increased gross system weight.

Figure 17 shows the typical variation of electrical conductivity as a function of potassium mass fraction in the flow. This curve was calculated utilizing LyTec's thermoequilibrium code which provides plasma electrophysical properties. The curve shown is for dynamic stated expanded from a 500 psia flame condition to 1 Atm static pressure.

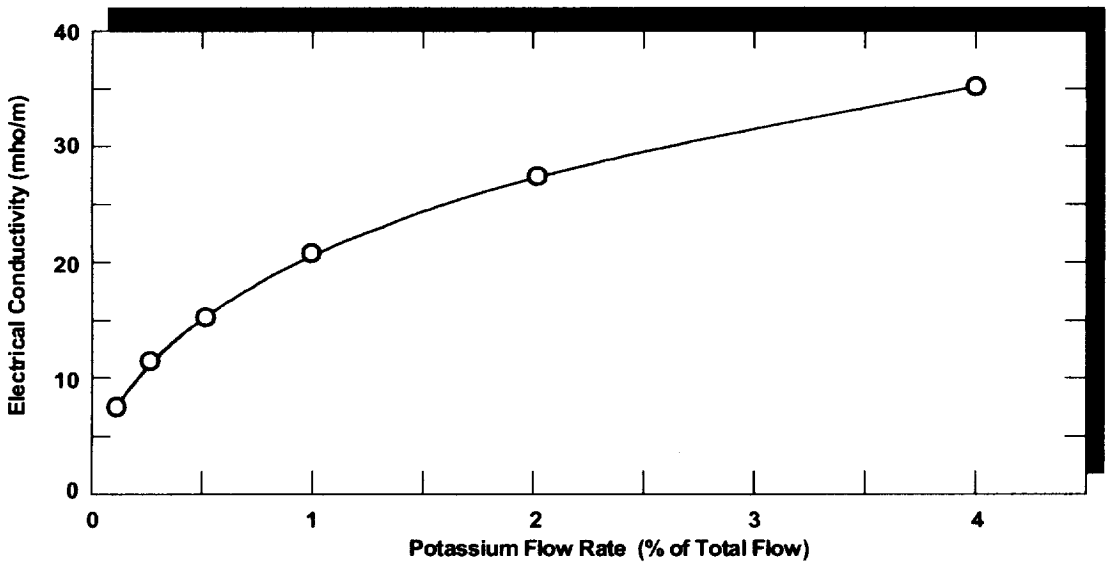

Figure 17. Variation of H2-O2 Combustion Gas Plasma Conductivity with K Seeding Percentage

Electrical conductivity is a very strong function of temperature since it determines the equilibrium energy distribution of electrons that are available for ionization. Conductivity is also a weaker, but significant, inverse function of pressure. Pressure affects the mean time between collisions of the free electrons with heavy molecules.

Another variable that affects the electrical conductivity of the plasma generated by the rocket motor with potassium addition is the stoichiometry of the H_2/O_2 combustion. This variation is illustrated in Figure18, which is calculated for 500 psia combustion at 1% potassium expanded to 1 Atm. The conductivity is seen to peak at about 95% stoichiometry. We chose to operate the rocket engine at a stoichiometry of 90% theoretical since we envision use some additional oxygen for transpiration cooling of the accelerator walls.

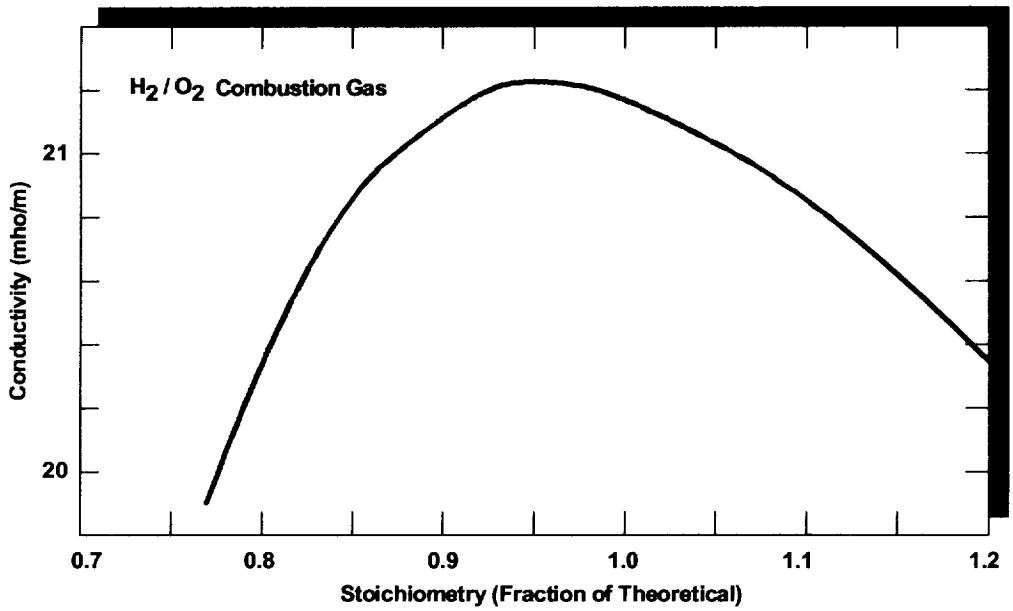

Figure 18. Variation of Plasma Conductivity with Combustion Stoichiometry

The MCRM concept consists of a rocket engine with nozzle truncated to provide the conditions for entrance into the accelerator (see Fig. 2). The accelerator may be designed (lofted) to control the internal plasmadynamic state variation along its length. A positive area gradient along the accelerator length increases the velocity of the supersonic flowing gas. At the exit of the accelerator, an additional gas dynamic nozzle may or may not be desirable to maximize exhaust velocity (Isp) by matching the exit pressure closely to the space environment back pressure.

A previous study [2] suggested that the MHD accelerator include all the area expansion to match pressure to ambient, however, design reliability considerations may dictate use of a nozzle in the very low pressure region. This is discussed later in our suggestions and recommendations for further optimization study of the system.

The choice of plasma thermodyamic state point at the accelerator entrance and its control through the accelerator provides a means for optimizing the MHD process. In our study, a

front-end analysis was accomplished to determine where to truncate the rocket engine nozzle to fix the inlet thermodynamic state for maximum MHD process effectiveness. Lineberry [24] has shown that the optimum entrance conditions for the MHD generator is at the Mach number that optimizes the power density. Power density is defined by the power density parameter, i.e.,

$$Pd = \sigma u^2 B^2,$$

where σ is the electrical conductivity, u is the velocity of the gas and B is the magnetic field flux density. Power density parameter is a property of the plasma. Its variation with expansion state arises from the relative "product" effect of decrease in temperature (or conductivity) versus increase in velocity squared during expansion.

The variation of this parameter with expanded MHD accelerator entrance state is shown in Figure 19. For the H_2-O_2 combustion gas plasma, the optimum Mach number was determined to be about 2.6.

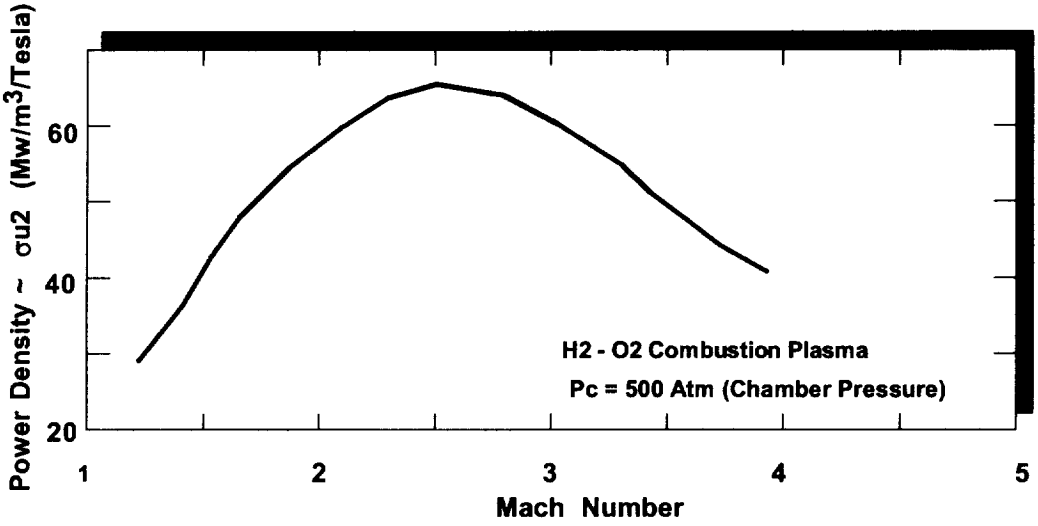

Figure 19. Variation in Entrance State Power Density with Mach Number

In certain accelerator applications, where the applied electrical power is not a constraint, beginning the accelerator at a lower Mach number can help facilitate more total acceleration. However, the most efficient acceleration possible is when this parameter is maximized.

For the principal cases reported in this study, the entrance was chosen at a Mach number of 1.8. That is, the converging-diverging nozzle of the rocket engine is truncated at the area ratio consistent with this Mach number. This inlet state point was used in most all calculations performed using LyTec's accelerator design and analysis code. With the observation made in this study of the overriding weight of the rectenna system, additional considerations and trade-offs need to be given to determine just what is the most effective overall accelerator system rather than maximizing the outlet velocity to maximize Isp.

4.2 Calculation Methodology

The calculation methodology used in this study is LyTec's one-dimensional MHD accelerator computer code which numerically solves the coupled the plasmadynamic equations discussed in Section 3. Detailed description of this code is contained in reference materials.[1-6] The code has been used in past studies by LyTec researchers on MHD accelerators in application to both wind tunnels and small scale MHD thrusters.

The model is subject to the following assumptions:

- The gas is homogenous in species concentration and thermodynamic properties.
- The gas is in chemical and thermodynamic equilibrium.
- The flow is uniform in a plane perpendicular to the flow.
- Induced magnetic fields are negligible.
- Plasma-to-electrode voltage drops are proportional to generated voltage (uBd)

The code has provisions to model gas dynamic and MHD electrical wall losses. Both friction and heat transfer are considered as well as boundary layer voltage drops. Heat losses and friction on the walls are calculated based on a correlation with the roughness height that is specified in the input. Boundary layer voltage drops can be computed locally based on boundary layer thickness and thermal profile, or, specified in accordance with Δ as defined in Section 3.1. Flow non-uniformity effects can be imposed by application of an appropriate estimate of Rosa's G-factor.[17]

The thermodynamic state of the plasma is determined by interpolation from a table of thermodynamic and electrical transport properties that are pre-calculated for the combustion gas products using the NASA SP-273 computer code or equivalent. The MHD accelerator code extracts thermodynamic (equation of state) and electrical transport properties needed for the calculation based on local pressure and temperature.

The code had provision to modeling the different MHD accelerator loading configurations (see Figure 16). In this study, only the Faraday configuration was considered. Loading was imposed by specification of the load factor, k, defined according to

$$k=Ey/uB$$

Moreover, load factor was specified as a function of distance along the accelerator (x coordinate) and a maximum current density was imposed. (That is, the load factor is used to calculate the required applied voltage until the resulting current density equals/exceeds the maximum specified; past this point, the applied voltage is calculated to give the specified current density.)

The computer code has provision for accommodating real magnetic field distributions. In this study a flat (constant intensity) magnetic field profile is specified.

There are three configurations for the accelerator that need to be considered for application to the MCRM. Figure 16 shows these different configurations including the Faraday, the diagonal and the Hall type accelerators.

The segmented Faraday accelerator consists of segmented electrode walls, i.e., discrete electrodes separated from each other in the longitudinal direction by insulators. The segmented Faraday configuration eliminates axial currents as there is no external return path (through the electrode wall). The segmented Faraday configuration has the advantage in being the most effective of the three alternatives in the sense that it can be controlled to optimum conditions by way of a separate power supply for each electrode pair. The latter characteristic is also a disadvantage in that it requires separate power supplies for each electrode pair.

The diagonal connection also has segmented electrode walls but they are connected at an angle with the vertical so that the connected electrodes (anode and cathode) are at the same potential. This is achieved by diagonalizing the external electrical connections along an angle defined by:

$$\cot \theta = - Ey/Ex$$

with θ measured with respect to the vertical. This diagonal arrangement allows both the axial (Hall) and transverse (Faraday) electric fields to be loaded and permits the application of power from end-to-end or along a smaller section of channel length. This avoids the large number of power supplies required for the segmented Faraday accelerator. The diagonal configuration is attractive for operating regimes in which this angle is reasonable for physical implementation.

The Hall configuration is a derivation of the diagonal where in the diagonalization angle is vertical. The Hall accelerator is attractive in the low pressure regimes where high Hall parameter (cyclotron frequency times the mean time between collisions) is high. This condition exists in the MCRM highly expanded, low density region of the accelerator operating to near vacuum condition.

The calculations made in this study use the Faraday configuration. This simplistic approach was used since it was within the resources made available to accomplish this initial study. We note that the performance of the Faraday configured accelerator in terms of acceleration to high velocity can achieved with other configurations. We further note, that opportunity to improve the simplicity and reliability of the MCRM can be achieved by using other configurations or combinations of configurations. For example, it appears that a diagonal connection for the upstream portion of the accelerator, followed by a Hall section downstream may simplify the system.

The set of equations governing the operation of the accelerator simplify to three equations in four unknowns, cross-sectional area, pressure, temperature and velocity along the channel. Thus, any one of the four variables can be specified and a design determined with the other three variables calculated. Based on previous experience with this methodology, the mode commonly used is to specify the internal flow dimensions of the

accelerator duct (area mode). In this study, the code is used iteratively to determine the area distribution and power application that yielded the desired accelerator performance.

4.3 Discussion of Results

A myriad of cases were calculated in our study. Table II gives a listing of a few typical cases that were calculated and quantifies some of the important performance parameters.

Table II Cases – MHD Accelerator Calculations

Case	Mdot kg/s	Bmax T	Power mW	Efficiency %	Jymax Amp/cm^2	Velocity m/s	Isp	Length m
1	2.2	2	777.3	80.8	30	24,496	2,500	1.2
2	2.2	4	725	88.6	16	24,648	2,515	1.2
3	2.2	6	702.1	90.8	12	24,451	2,495	1.2
4	2.2	8	740.7	92.3	10.2	25,216	2,573	1.2
5	5	4	1,650	88.7	16	24,680	2,518	1.2
6	5	2	1,776	80.6	31	24,529	2,503	1.2
7	10	4	3,230	88.5	16.3	24,491	2,499	1.2
8	2.2	4	707.3	90.5	9	24,476	2,498	2.4
9	0.022	8	6.7*	89	5	23,970	2,446	1
10	0.022	4	6.8*	85.7	10	23,743	2,423	1

* Add 350 kW if water is used for fuel instead of H2-O2

The base case (suggested by NASA ASTP experts) around which parameteric studies were formed was for a mass flow rate of 2.2 kg/s. (As discussed in Section 3.0, the Isp achieved is proportional to the square root of the applied power and the weight of the rectenna system varies as the first power. This fact implied that the optimum utilization regime for the beamed power, MCRM system is in lower size systems based upon the projected specific power for contemporary rectennas.) Higher mass flows were also computed as noted in the Table. The last two cases were calculated for a very low mass flow rate, 0.022 kg/sec.

We annotate the following points:

- None of these calculated results are unique. For example, a longer length can be used with a lower current density to achieve the same acceleration at a slightly reduced efficiency.
- In all cases, choosing different inlet conditions to the accelerator will affect the detailed results.
- There is a high probability and need for further optimization of the accelerator, depending upon the optimization criteria one selects.

In the first four cases of Table II, the magnetic field flux density was varied from 2.0 to 8.0 Tesla for a fixed mass flow rate of 2.2 kg/s. The accelerator was loaded to achieve an Isp of approximately 2,500 seconds over a 1.2 meter total length (including exhaust nozzle). As tabulated, the efficiency increases with magnetic field. This behavior is

because the accelerating force is proportional to current density times magnetic field flux density. Therefore, at a higher magnetic field, proportionally less current is required and the resistive power dissipation in the plasma decreases as the square of the current density. The efficiency shown in Table II is the 'electrical efficiency' as defined in Section 3.1. This represents the ratio of work done on the gas by MHD force to the electrical power input. It should be pointed out that the electrical losses go to heating the gas which also has a second order propulsion benefit.

The estimated weight of the magnet increases from 845 kg for the 2 Tesla case to 988 kg for the 8 Tesla case. Weight of the entire MHD accelerator including magnet, channel and subsystems for these two extreme power density cases varied from 1,209 kg at 2 Tesla to 1,252 kg at 8 Tesla. The heaviest MHD system calculated was the large 10kg/sec flow rate (Case 7) at 2,115 kg. The non-linear character in system weight arises from variations in MHD accelerator size and power density (i.e., the same power level for acceleration can be achieved in a smaller size accelerator as the magnetic field increases).

In cases 4, 5 and 6, higher mass flows were explored to view scale-up issues. These cases show how power requirement vary with mass flow rate - reaching more than a gigawatt for the 5 kg/sec case. The electrical efficiency shown does not reflect overall thermodynamic efficiency which improves with size, i.e., a reduction in the surface to volume ratio.

Case 8 at 2.2 kg/s was intended to show the design option of operation at reduced (1/2) the power density by making the accelerator twice as long. Although the wall losses increase and the overall weight of the MHD propulsion system increases, it is clearly feasible to utilize this design trade-off to scale down the interaction level as needed for reliability and still maintain a very effective system.

The last two cases (9 and 10) are at a very low mass flow rate, 0.022 kg/s. These cases were calculated because system/mission analyses based on high rectenna weights scaled on a linear basis with power, indicate that a near term attractive regime for MHD augmentation is at small scale. These cases were expanded further in the rocket motor nozzle before entering the MHD accelerator in order to achieve an increase the physical size of the flow channel. However, more detailed calculations, especially in treatment of boundary layer growth and losses, are needed to be assured that this small size is feasible.

The footnote of Table II indicates the additional power required if direct heating of water (actually ice) is used as the working fluid for the propulsion system instead of hydrogen/oxygen rocket engine. This option has been suggested by NASA ASTP propulsion experts and it should produce a weight saving in the tankage required for the system and be compatible with a water fuel concept.

Typical distribution plots generated for the 10 kg/s calculation are provided in Figures 20 and 21. Figure 20 presents distribution along the channel length of control variables and gas/plasma dynamic properties. Figure 21 presents similar distributions for electrical and energy balance performance terms. This set of calculations consisted of a 1.2 meter accelerator channel without a exhaust expansion nozzle.

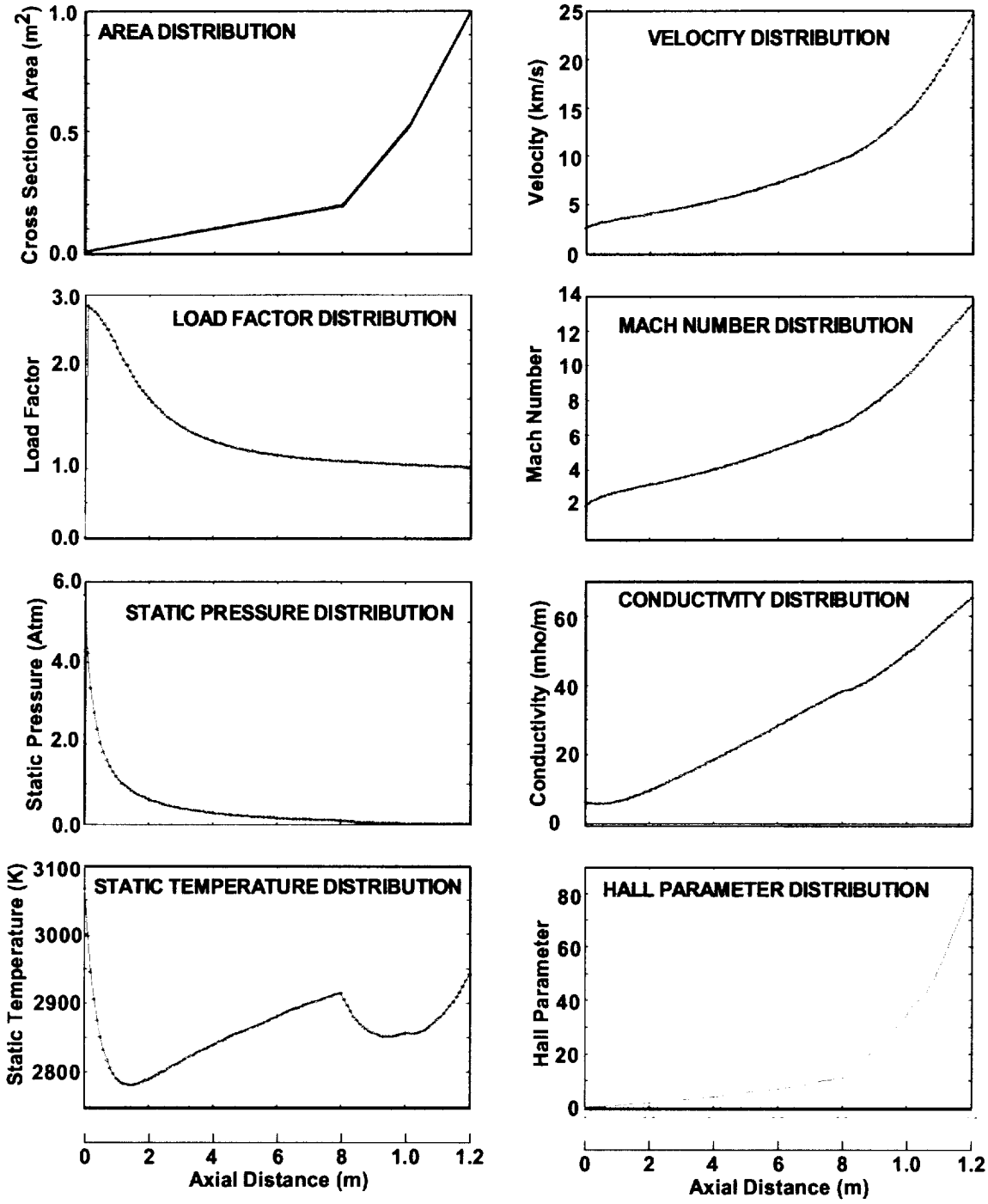

Figure 20. Typical Calculation Results – Distributions of Variables Along the MHD Accelerator Length

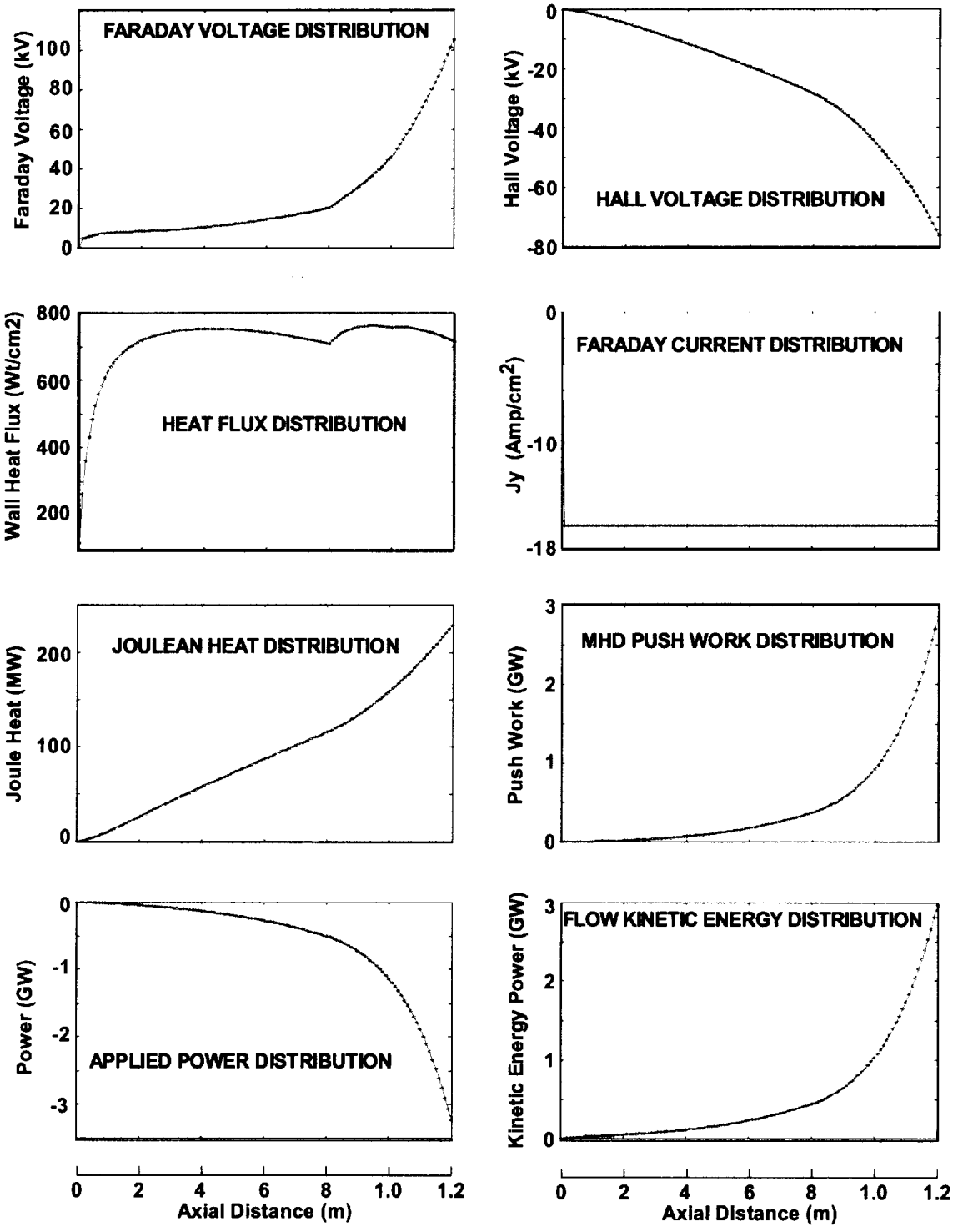

Figure 21. Typical Calculation Results – Distributions of Energy and Electrical Variables Along the MHD Accelerator Length

For the most part, the plots of Figures 20 and 21 are self-explanatory. A few observations on these plots are noted here for the record.

- These calculations are meant to be representative and do not present any design recommendations. In general, the flexibility of the 1-D calculation methodology allows the presence of large axial gradients to exist independent of any known true, physical restrictions.
- These calculations are subject to the imposition of thermal equilibrium chemistry. Other 'parallel' calculations were made considering frozen kinetics for comparison. These calculations were in general agreement within 10% in the acceleration effectiveness.
- The ability of the thermochemical equilibrium code to properly predict the gas and plasma properties in the very low density regime (low pressure regions) is an uncertainty. Generally speaking, in the far downstream nozzle region, at the high temperature achieved, most all species become atomic implying that non-equilibrium ionization will exist.
- The expansion ratio as shown is considered is quite large and may be unrealistic for a real design. This distribution was utilized to optimize/maximize the Isp over a short length. However, one does observe that the MHD acceleration process lends strong positive gradients in both pressure and temperature. In a system optimized for operation, a longer span would probably better serve to accommodate the large expansion ratio.
- The design chosen is very close to being operation at constant temperature. Only a variation of 200K across the accelerator is seen. The noticeable inflection in temperature seen at the 0.8 m location is consistent with the area inflection point. The character of maintaining high temperature with in the accelerator assures elevated conductivity throughout the channel lending efficiency to the MHD processes.
- The extremely high Hall parameter that are associated with MCRM operation to low back pressure is demonstrated in these results.
- Similarly, an extremely high Hall voltage that builds up across the accelerator's length. We recognize that this level of Hall field gradient cannot be accommodated with this Faraday design since axial electrical breakdown between electrodes can be expected. Constraints on the Hall voltage gradient need to be applied in future calculations.
- The plots of Figure 21 that show the energy distributions and fluxes illustrate the conservation of energy as applied to the various terms of the MHD accelerator.

5.0 CONCLUSIONS AND RECOMMENDATIONS

The study and results presented herein are to be considered as a preliminary "first look" at the new concept being considered by NASA ASTP in application of beamed energy to drive a MCRM. This effort was extensive in our attempt to consider all aspects of the problem. It was also limited in both the time available to accomplish this effort and in the resources with which to accomplish it.

We contend that a fairly thorough "first look" is provided in the contents of this report. We also express our desire to continue this work to allow us to examine some of the technical points that were brought up herein with regard to system constraints and system optimization.

In the following, we provide bulleted statements that highlight major conclusions drawn from this work. Other important findings are contained within the body of this document. We also provide recommendations for areas that we consider as future needed efforts related to the MCMR and to the specific beamed energy, boost-to-escape mission.

CONCLUSIONS

- The MHD augmented rocket propulsion system (MCRM) is promising for boost from orbit of a deep space vehicle that can be powered by microwave power from an orbiting power station. Very high specific impulse and simultaneous with high thrusts are plausible with MHD accelerator propulsion. Further work is needed to fully qualify this mission in terms of size, scope and detailed design needs. The beamed energy driven MCRM concept represents an advanced propulsion system that could significantly improve space transportation capability by lending high performance thrusters for deep space and inter-planetary missions.

- Current and predicted technology advances in materials and subsystems needed for the MCRM are most promising. From our literature reviews, we contend that light weight, high temperature superconducting magnets could well be as close as a decade away from being a reality. Similarly, light weight, high strength materials based on carbon nano-tube technology and composites are near term. In general, the principal facet that has plagued used of MHD propulsion in the past "Weight" will soon come to pass lending this system a leader for advanced space propulsion.

  Furthermore, we emphasize that our study on the beamed energy mission application revealed that the weight of the MHD system was insignificant in comparison to the weight of the rectenna.

- The pacing technology for the beamed energy driven MCRM (and other beamed energy advanced propulsion concepts under study by NASA) is the rectenna specific power. The weight of the rectenna based on contemporary estimates of these devices power density (1.0 to 4.0 kw/kg) far exceeds that of the total MHD system. The rectenna specific power is the controlling factor on what scale the

MCRM is plausible – with smaller scale systems being shown applicable to contemporary rectennas specific power projections.

For the beamed energy driven MCRM propulsion system to be applicable for large scale inter-planetary missions, improvements in rectenna specific power of an order of magnitude or more are needed. Other novel, actively cooled rectenna design concepts need to be explored.

- Algorithms were developed to predict the weight of the MHD accelerator including the magnet, channel, power conditioning equipment and seeding system. Optimistic figures were used for this engineering effort considering advanced superconductors and advances in light weight, high strength materials. The MHD accelerator system weight was dependent upon the size of the MHD accelerator which was in turn dependent upon its operation (trade-offs in throughput, magnetic field intensity, and operating current). However, the MHD accelerator system weight (< 0.25 mTon) was determined to be insignificant in comparison to that of the rectenna.

- MHD acceleration scales to higher efficiency, lower weight per unit of thrust and lower cost per unit of thrust with larger size.

- The efficiency of the MHD accelerator depends on design parameters such as magnetic field strength, length, scale and operating regime. A conservative estimate of efficiency is 80%, with the electrical losses going into heating the working fluid which also benefits the accelerator.

- Effective utilization of an MHD accelerator in space leads to very low static pressure in the downstream end of the accelerator, high Hall parameters and high axial potential. These conditions favor/require the utilization of a diagonal or Hall configured accelerator. These configurations can be designed to produce substantially the same performance as calculated in this study.

- Considerations need to be given to non-equilibrium MHD accelerator designs in recognition of the low pressure operating regime in which the space based system will operate. Taking advantage of non-equilibrium ionization in the extremely low density plasma that occurs with high expansion, provides a potential means for reducing power requirement and further enhancing the acceleration performance of the MCRM.

- The MHD system is amenable to different working fluids, including H_2/O_2 engines, solid fuels with or without separate oxidizing agents and water. Different propellants and combinations need to be explored for MCRM application.

- The reliability and lifetime of the MHD accelerator is a function of power density, operating potentials and cooling methods. All of these variables can be designed to be within limits needed for required reliability.

- There is a deficit of knowledge and experience in MHD accelerator technology that plagues design issues related to the MCRM. No experimental work on the MHD accelerator has been done in the U.S since the 1960's.

RECOMMENDATIONS FOR FURTHER WORK

- Research work on the development of a lightweight rectenna system for use at the high frequencies suitable for space propulsion and at higher power densities should be accelerated, in support of both the MCRM under study herein and other NASA advanced propulsion initiatives.

- The use of a Hall configured accelerator should be explored both computationally and experimentally. LyTec has available the computational methods to perform this effort.

- Exploration of non-equilibrium ionization for MCRM operation is another area that needs evaluation. Taking advantage of use of a non-equilibrium plasma may well reduce the power requirements by two fold.

- An experimental research facility for MHD acceleration research and development needs to be established. This facility can be moderate in scale and dedicated to the study of basic physics phenomena; such as, energy deposition definition, flow non-uniformity issues, current transport (diffuse versus arc), electrode reliability, electrical conductivity measurements, power density effects and other similar issues can be explored and validated.

6.0 REFERENCES

1. Crawford, R. A., J. N. Chapman and R. P. Rhodes, "Potential Application of Magnetohydrodynamic Acceleration to Hypersonic Environmental Testing", Proceedings of the 33rd Symposium on the Engineering Aspects of MHD, AEDC-TR-90-6, Final Report, August 1990.
2. Crawford, R. A., Chapman, J. N., and R. P. Rhodes, "Performance Potential and Technology Issues of MHD augmented Hypersonic Simulation Facilities, "AOAA-90-1380, AIAA 16th Aerodyn;amic Ground Testing Conference, June, 1990
3. Lineberry, J. T. and R. A. Crawford, "The MHD Accelerator", *Mechanical Engineering*, Vol. 113, No. 9, September 1991.
4. Lineberry, J. T. and J. N. Chapman,"MHD Accelerators for Hypersonic Applications", AIAA-91-0384, 29th AIAA Aerospace Sciences Meeting, Reno, NV, January 1991.
5. Chapman, J. N., J. T. Lineberry, and H. J. Schmidt, "Application of MHD Accelerators to Hypersonic Ground Test Facilities", *Proceedings of the 28th Symposium on Engineering Aspects of Magnetohydrodynamics*, June 1990.
6. Schulz, R. J., Chapman, J. N., and R. P. Rhodes, "MHD Augmented Chemical Rocket Propulsion for Space Applications," AIAA-92-3001, AIAA 23rd Plasmadynamics and Lasers Conference, July, 1992.
7. Schulz, R. J. and J. N. Chapman, "Optimum Performance of MHD-Augmented Chemical Rocket Thrusters for Space Propulsion Applications", Proceedings of the 33rd Symposium on the Engineering Aspects of MHD, University of Tennessee Space Institute, Tullahoma, TN, June 1995.
8. Power, John L., "Microwave Electrothermal Propulsion for Space", IEEE Transactions on Propulsion in Space", Vol. 40, No. 6, June 1992.
9. Frisbee, R. H., et al, "Advanced Propulsion Options for the Mars Cargo Mission", AIAA/SAE/ASME/ASEE 26th Joint Propulsion Conference, Orlando, RL, AIAA 90-1997, July 16-18, 1990.
10. Sercel, Joel C. and Robert H. Frisbee, "Beamed Energy for Spacecraft Propulsion", Proceedings of the Princeton/AIAA/SSI Sixth Conference on Space Manufacturing, pp252-265, 1987.
11. Koert, Peter and James T. Cha, "Millimeter Wave Technology for Space Power Beaming", IEEE Transactions on Microwave Theory and Technology, Vol 40, No 6, pp1251-1258, June 1992.
12. Brown, William C. and E. Eugene Eves, "Beamed Microwave Power Transmission and its Application to Space", IBID, pp1239-1250.
13. Glazer, Peter E., "Overview of the Solar Power Satellite Option", IBID, pp 1230
14. Sercel, J. C., "Microwave Electric Propulsion for Orbital Transfer Applications," in JANNAF Joint Propulsion Conference Transactions, San Diego, California, April 9-12, 1985.
15. Alfyorov, V.I., "Current State and Potentialities of Hypersonic MHD-Gas Acceleration Wind Tunnels", Lecture at U. S. Air Force Arnold Engineering Center, November, 1997.
16. Brogan, T. R., "The 20MW LORHO MHD Accelerator for Wind Tunnel Drive – Design, Construction and Critique," AIAA-99-3720, 30th Plasmadynamics and Lasers Conference, June, 1999.
17. *Magnetohydrodynamic Energy Conversion*, R. J. Rosa, McGraw-Hill, 1968.
18. A. T. Carter, et. al., "Operating Characteristics, Velocity, Pitot Tube Distribution, and Materials Evaluation Test in the Langley One-Inch-Square Plasma Accelerator," AIAA Plasmadynamics Conference, March 2-4,1966.

19. L. E. Ring, "General Considerations of MHD Acceleration for Aerodynamic Testing," AGARD Specialist's Meeting on Arc Heaters and MM Accelerators for Aerodynamic Purposes, Rhode-Saint-Genese, Belgium, 1964.
20. K. E. Templemeyer, L. E. Rittenhouse, and D. R. Wilson, "Experiments on a Faraday-Type MHD Accelerator with Series Connected Electrodes,' AIAA Journal, Vol. 3, No. I 1, September 1965.
21. Technology Development and Assessment Program for MHD Augmented Hypersonic Test Facilities," NASA Report, MSE, Inc., February 1994.
22. Litchford, R. J., V. A. Bityurin, and J. T. Lineberry, "Thermodynamic Analysis of the AJAX Propulsion Cycle," AIAA 2000-0445, Jan 2000.
23. Bityurin, V. A., Lineberry, J. T., "MHD Augmented Hypersonic Propulsion Systems," 1st International Workshop on Perspectives of Plasma and MHD Aerospace Technologies, Moscow, 1998.
24. Lineberry, J. T.,"MHD Generator Optimization", Simulation and Design of Applied Electromagnetic Systems, Elsevier Studies in Applied Electromagnetics in Materials, pp 723-726, Elsevier Press, 1994.